

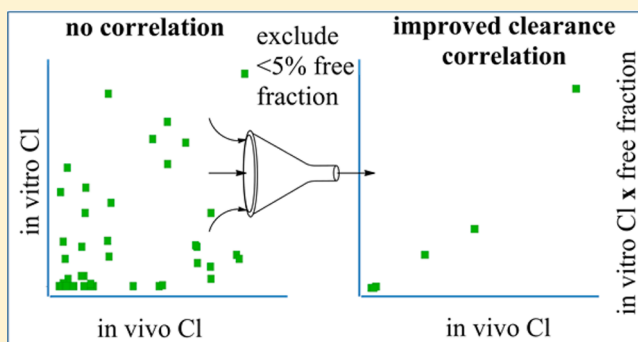
Reductions in log P Improved Protein Binding and Clearance Predictions Enabling the Prospective Design of Cannabinoid Receptor (CB1) Antagonists with Desired Pharmacokinetic Properties

Bruce A. Ellsworth,* Philip M. Sher, Ximao Wu, Gang Wu, Richard B. Sulsky, Zhengxiang Gu, Natesan Murugesan, Yeheng Zhu, Guixue Yu, Doree F. Sitkoff, Kenneth E. Carlson, Liya Kang, Yifan Yang, Ning Lee, Rose A. Baska, William J. Keim, Mary Jane Cullen, Anthony V. Azzara, Eva Zuvich, Michael A. Thomas, Kenneth W. Rohrbach, James J. Devenny, Helen E. Godonis, Susan J. Harvey, Brian J. Murphy, Gerry G. Everlof, Paul I. Stetsko, Olafur Gudmundsson, Susan Johnghar, Asoka Ranasinghe, Kamelia Behnia, Mary Ann Pelleymounter, and William R. Ewing

Research and Development, Bristol-Myers Squibb, Co., P.O. Box 5400, Princeton, New Jersey 08543-5400, United States

S Supporting Information

ABSTRACT: Several strategies have been employed to reduce the long in vivo half-life of our lead CB1 antagonist, triazolopyridazinone 3, to differentiate the pharmacokinetic profile versus the lead clinical compounds. An in vitro and in vivo clearance data set revealed a lack of correlation; however, when compounds with <5% free fraction were excluded, a more predictable correlation was observed. Compounds with log P between 3 and 4 were likely to have significant free fraction, so we designed compounds in this range to give more predictable clearance values. This strategy produced compounds with desirable in vivo half-lives, ultimately leading to the discovery of compound 46. The progression of compound 46 was halted due to the contemporaneous marketing and clinical withdrawal of other centrally acting CB1 antagonists; however, the design strategy successfully delivered a potent CB1 antagonist with the desired pharmacokinetic properties and a clean off-target profile.



INTRODUCTION

The cannabinoid receptor 1 (CB1) is a G-protein-coupled receptor (GPCR) with high expression in the central nervous system (CNS) that promotes feeding when activated by endogenous cannabinoid agonists such as anandamide and 2-AG.¹ The CB1 receptor antagonist, rimonabant (SR141716), which had been marketed in Europe as Acomplia for the treatment of obesity, binds to the human CB1 receptor with nanomolar affinity and blocks signaling of the receptor.² In the RIO clinical trials in North America and Europe, 20 mg qd of rimonabant was shown to reduce body weight of obese subjects by ~4.7% over placebo during the first year of treatment. This weight loss was then maintained over the second year of treatment.³ Rimonabant was withdrawn by Sanofi SA from consideration for regulatory approval by the FDA in the U.S., and its marketing was voluntarily suspended in Europe. The European Commission later withdrew marketing authorization due to psychiatric side effects.⁴

The structures of CB1 antagonists have been reviewed;⁵ however, there are only a few reports that describe efforts to affect in vivo clearance of CB1 antagonists via changes in log P. Letourneau et al. have described their efforts to reduce

metabolism within their chemical series via reduction in log P from 5.6 to 4.6, resulting in an improved microsomal stability.⁶ Griffith et al. reported the discovery of otenabant via reductions in log P relative to rimonabant (ϵ log D = 4.0 vs 5.8) that led to greater microsomal stability and low metabolic clearance.⁷ While those efforts to reduce log P were employed to increase half-life, we wished to reduce the long in vivo half-life of our lead CB1 antagonist 3 in an attempt to provide a differentiated pharmacokinetic (PK) profile versus other CB1 antagonists.

The most clinically advanced CB1 antagonists, rimonabant, taranabant, and otenabant, exhibit long elimination half-lives ($T_{1/2}$ of 9–15 days, 3–4 days, and 5–8 days, respectively)^{8–10} in humans. Compounds with long elimination half-lives may add significant time and expense to early clinical trials, and there may be significant delay in drug withdrawal for patients experiencing adverse events.¹¹ Drug accumulation to steady-state and drug washout studies typically require 4 times $T_{1/2}$,¹² as demonstrated by the reported 13 days required for taranabant to reach steady state and 28 day monitoring of

Received: July 17, 2013

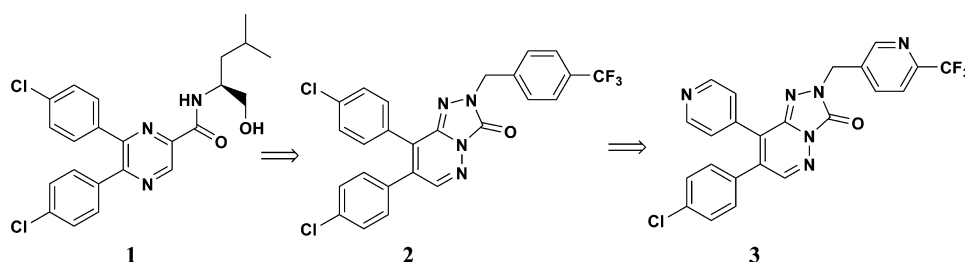


Figure 1. Evolution of the triazolopyridazine series of CB1 receptor antagonists.

drug elimination for otenabant in human PK studies.^{9,10} Whereas a single-dose PK assessment can be made for compound with a 12 h half-life with 4 days of monitoring, it may take as much as 120 days of monitoring for each dose level of a compound with 15 day half-life. Furthermore, there is a significant delay in drug clearance in the event of an adverse event.¹² For example, diazepam (washout half-life of 79 h) exhibited fatigue and sedation side effects 2 weeks after drug withdrawal while oxazepam (washout half-life of 10.7 h) side effects subsided rapidly after drug withdrawal.¹³ By developing a CB1 receptor antagonist with a shortened elimination half-life, it was hoped that our early clinical program would move quickly and that rapid drug washout would improve safety in the case of reversible adverse events. To accomplish this goal, herein we describe efforts to discover potent and selective CB1 antagonists with predictable half-life using medicinal chemistry principles that may be applicable beyond the field of CB1. These strategies may be useful when applied to other lipophilic receptor ligands that have high MW or log P, leading to long in vivo half-life.

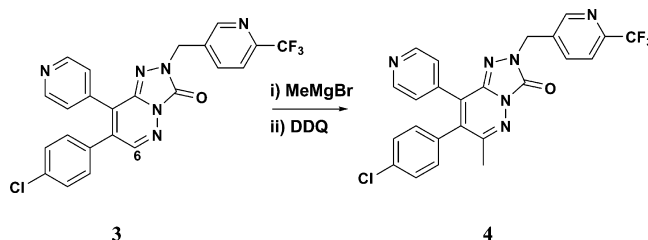
RESULTS AND DISCUSSION

Our lead series of CB1 antagonists originated from high-throughput screening (HTS) hits and evolved through a series of pyrazine carboxamides (**1**, Figure 1) as reported previously.¹⁴ To lower log P and improve physicochemical properties¹⁵ (e.g., aqueous solubility), we explored alternative cores, resulting in the discovery of the triazolopyridazine (TZP) series.¹⁶ An effort to replace two chlorophenyl substituents and the benzyl group of compound **2** revealed that pyridine groups in compound **3** conferred the desired solubility and log P improvement while maintaining good human CB1 receptor (*hCB1*) binding affinity. Compound **3** was found to have a long half-life in all species tested ($T_{1/2}$ = 15, 108, and 26 h in rat, dog, and monkey, respectively),¹⁷ so the medicinal chemistry effort focused on an attempt to maintain the compound's positive characteristics while decreasing in vivo half-life.

In an effort to introduce a methyl group as a metabolic soft spot, methyl magnesium bromide was found to add to the 6-position of the TZP ring which, upon rearomatization by air or DDQ, led to the formal replacement of methyl for hydrogen at the C6-position (Scheme 1).¹⁸ Unfortunately, an alkyl substituent at this position significantly decreased in vitro affinity (compound **4** vs **3**, Table 1). In contrast, a methoxy group at this position (compound **5**, Table 1) was equipotent in vitro to compound **3**. Compound **7**, an *O*- to *N*-methyl isomer of **5**, was also a potent CB1 antagonist. These compounds, however, did not yield desired improvements of in vivo efficacy or half-life in rats vs compound **3**.

We found that the N5-position (X = N) could tolerate significantly larger substituents than the simple methyl group as

Scheme 1. Methyl Grignard Addition to Triazolopyridazinone **3**

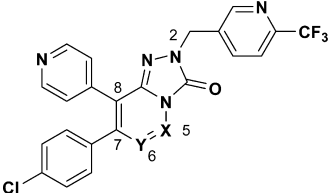


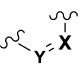
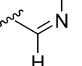
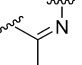
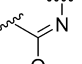
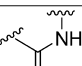
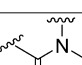
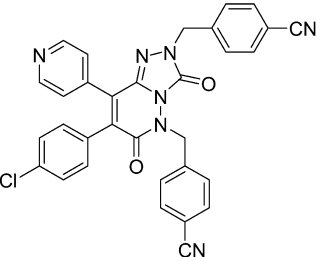
found in compound **7**. For example, compound **8** (Table 1) provided encouragement that there may be a new binding pocket that could be exploited. Having extensively searched for polar moieties to replace the N2-lipophilic CF₃-benzyl group of compound **2** with limited success,¹⁶ we hoped we could exploit this new pocket to introduce a polar substituent at N5. We started this exploration with two central tenets: (1) the C8-pyridine moiety of compound **3** had brought several favorable traits, including polarity, so we wished to incorporate a pyridine or a suitable substitute and (2) we chose to minimize the substituent in the N2-pharmacophoric space because large hydrophobic moieties counteracted the benefits of the polar C8-pyridine moiety. Transposition of the C8 pyridine and the C7 chlorophenyl groups, a product that was synthesized as the result of a nonregioselective route, led to greater affinity for compound **11** as compared to compound **10** (Figure 2).

As we explored the SAR of the N5-benzyl substituent in this transposed series, we found similar activity trends to that exhibited by the N2-benzyl compounds in the original series, suggesting that the two isomeric structures may be occupying the same binding pockets in the CB1 receptor, as depicted in Figure 3. As further support for this hypothesis, mutagenesis studies reveal that compound **11** and compound **3** lose 20–40-fold binding affinity against mutant F200A while the affinity is recovered in mutant F200L, suggesting similar interactions with the CB1 receptor.²¹ While that observation argued against the likelihood of finding more potent polar substituents at N5 of compound **12**, it was immediately recognized that the properties of the transposed triazolopyridazin-diones (TZP-diones) were favorable despite bearing the same substituents. With some sacrifice of in vitro affinity, we found significant improvement in crystalline aqueous solubility (40 vs 1 $\mu\text{g/mL}$ for **12** and **7**, respectively) as well as desired reductions of in vivo half-life in rats (6 vs 35 h for **12** and **7**, respectively).

Capitalizing upon the SAR of the earlier TZP series, incorporation of a 6-methyl-2-trifluoromethylpyrid-3-yl side chain increased affinity by ~2–3-fold (compound **13**) and a slightly larger N2-alkyl substituent (compound **15**) further improved CB1 binding affinity (Table 2). Compound **15** was efficacious in reducing food intake by 43% acutely,²⁰ and in a 4-

Table 1. Pharmaceutical Properties of Pyridazinone Core Substitutions



	Cmpd #	<i>h</i> CB1 <i>K_i</i> (nM)	S.D. (nM)	<i>e</i> log P ^a	MED ^b in rats @ 20 h	Rat <i>T</i> _{1/2} [CI] (mL/min/kg) ^c
	3	12	4.5	3.2	0.3 mg/kg	15 h [0.4]
	4	210	68	3.3	n.d.	n.d.
	5	10	4.7	3.7	3 mg/kg	17 h [1.1]
	6	4000	1200	2.5	n.d.	n.d.
	7	18	12	3.5	1 mg/kg	35 h [0.40]
	8	4.2	1.3	4.6 ^d	n.d.	n.d.

^aThe term “*e* log P” refers to experimentally measured log P.¹⁹ ^bMED represents the minimally efficacious dose that produces statistically significant food reduction in nonfasted rats feeding ad libitum over a 20 h period.²⁰ ^cTerminal half-life (*T*_{1/2}) and clearance [CI] were measured in Sprague–Dawley rats upon iv administration of 3 mg/kg of test compound. ^dLog P was not measured for this compound; calculated log P of compound 8 is 4.6.

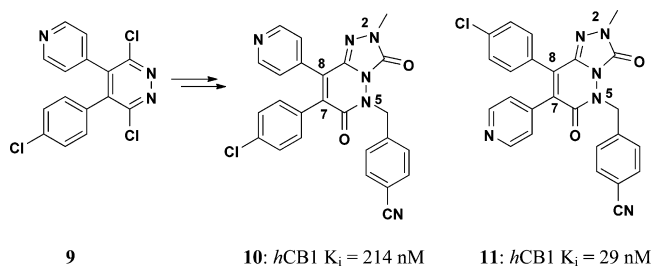


Figure 2. SAR of 4-pyridine positional isomers.

day study²² it reduced body weight by 4% when administered qd at 10 mg/kg to ad libitum fed rats (resulting in plasma

concentrations of 4 μM at *C*_{max} and AUC_{0–24} = 48 μM h). In the same study, rimonabant gave 5% body weight reduction when administered at 10 mg/kg qd. Several liabilities had been resolved at this point: compound 15 displayed good in vitro affinity and in vivo efficacy while maintaining relatively low log P and shortened in vivo half-life relative to compound 3.

Compound 15 was synthesized according to the sequence depicted in Scheme 2. Commercially available 4-pyridylacetic acid was *O*-alkylated with bromide 17, followed by cyclization to butenolide 18. Base-catalyzed air oxidation generated anhydride 19 and reaction with hydrazine gave pyridazinone 20. Dehydrative chlorination of 20 was achieved with POCl₃ to give pyridazine dichloride 9. Displacement of

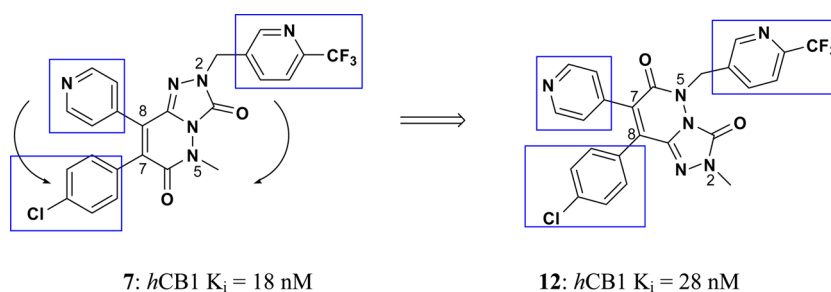


Figure 3. Comparison of proposed binding modes and of *hCB1* K_i values for *N*-2- CF_3 -pyridyl- vs *N*-5- CF_3 -pyridyl-triazolopyridazinediones **7** and **12**.

Table 2. SAR of Pyridyl-Containing TZP-diones

R	compd	<i>hCB1</i> K_i (nM)	SD (nM)	MED in rats @ 8 h ^a (% redn)	rat $T_{1/2}$ [Cl] (mL/min/kg)	CYP isoform IC_{50} (μM) ^b
$R_1 = \text{H}$ $R_2 = \text{Me}$	12	28	9.3	3 mg/kg (21%)	6 h [13]	2C19 = 4.3 2C9 = 1.9 3A4 = 6.6
$R_1 = \text{Me}$ $R_2 = \text{Me}$	13	9.0	4.3	3 mg/kg (33%)	3.3 h [6.3]	2C19 = 0.7 2C9 = 2.9 3A4 = 6.8
$R_1 = \text{H}$ $R_2 = \text{Et}$	14	15	6.9	n.d.	2.4 h [37]	2C19 = 11 2C9 = 4.9 3A4 = 18
$R_1 = \text{Me}$ $R_2 = \text{Et}$	15	4.5	1.5	10 mg/kg (51%)	5 h [9.9]	2C19 = 2.6 2C9 = 4.2 3A4 = 9.1 ^c

^aDue to shorter in vivo half-life, MED was determined at 8 h instead of 20 h. ^bMaterials and methods for CYP inhibition assays are found in the Supporting Information. ^cCYP 3A4 inhibition study in human liver microsomes. Upon re-evaluation in hepatocytes, compound **15** CYP 3A4 IC_{50} = 3 μM .

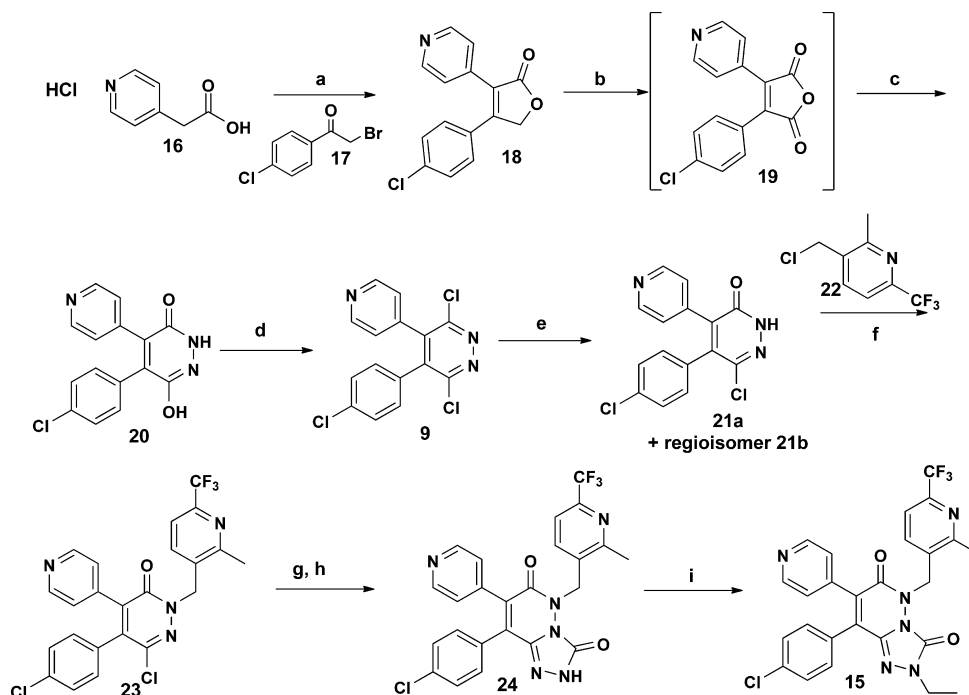
dichloride **9** was effected with NaOH, resulting in a separable mixture of regioisomers. Alkylation of **21a** with 3-(chloromethyl)-2-methyl-6-(trifluoromethyl)pyridine gave chloride **23**. The triazolo-ring was formed via chloride displacement with hydrazine and cyclization with 1,1'-carbonyldiimidazole to give bicyclic intermediate **24**. Alkylation with ethyl iodide completes the 9-step linear sequence, enabling the synthesis of several grams of compound **15** for advanced efficacy and safety studies.

Several liabilities were discovered during the preclinical in vitro and in vivo characterization of compound **15**. CYP inhibition was a concern because efficacy in humans was predicted to require micromolar plasma exposures of **15**. In higher species PK studies, compound **15** was also shown to have variable (15–50%) bioavailability and medium to high clearance.²³ Allometric scaling led to a predicted high clearance (39 mL/min/kg) in humans. While the goal of this program was to deliver a compound with shortened half-life (relative to

compound **3**), compound **15** was predicted to overshoot this goal.

Confident that a sufficiently short half-life was possible, we set out to identify a compound with appropriate half-life and bioavailability for predicted qd administration in humans while eliminating the CYP inhibition liability observed for compound **15**. We discovered SAR (Table 3), suggesting that the 4-pyridyl group of compound **15** was associated with CYP inhibition, but a 4-cyanophenyl derivative (**28**) displayed increased in vitro affinity as well as reduced CYP inhibition. However, substitution of a 4-cyanophenyl for a 4-pyridyl group at C7 ran counter to the program goals of decreased log P (4.6 vs 3.9) and increased solubility,²⁴ and this compound also displayed unacceptably long elimination half-lives in dogs (70 h) and cynomolgous monkeys (40 h).

In an attempt to introduce a metabolic soft spot to reduce its in vivo half-life, we incorporated a methyl group at various positions on compound **28**. Most of the derivatives in Table 4 had undesirable levels of *hCB2* binding IC_{50} s from 77 to 400

Scheme 2. Synthesis of Compound 15^a

^aConditions: (a) KOTBu, DMF, 88%; (b) air, KOTBu, THF; (c) hydrazine hydrate, EtOH, HCl, 32% (2 steps); (d) POCl₃, 85 °C, 72%; (e) NaOH, CH₃CN, 75%; (f) K₂CO₃, DMF, 66%; (g) hydrazine (anhyd) pyridine; (h) 1,1'-carbonyldiimidazole, THF, 73% (2 steps); (i) EtI, K₂CO₃, DMF, 67%.

Table 3. CB1 and CYP Isoform SAR of C7-Aryl-triazolopyridazinediones

Ar	R ₁	compd	<i>h</i> CB1 K _i (nM)	SD (nM)	<i>e</i> log P	CYP isoform IC ₅₀ (μM)
4-pyridyl	H	14	15	6.9	4.0	2C19 = 11 2C9 = 5 3A4 = 18
4-pyridyl	Me	15	4.5	1.5	3.9	2C19 = 3 2C9 = 6 3A4 = 3
3-methyl-4-pyridyl	Me	27	8.4	3.5	4.2	2C19 = 32 2C9 = 5 3A4 = >40
4-cyanophenyl	Me	28	1.4	0.58	4.6	2C19 > 40 2C9 > 40 3A4 > 40

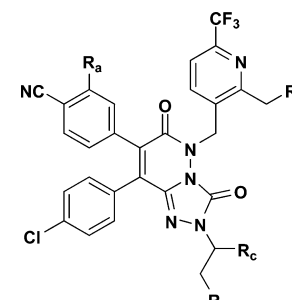
nM, making them undesirable for progression, but two compounds within the table (28 and 32) highlight a disconnection that became apparent (vide infra, Figure 4A) more broadly for the chemotype: that in vitro metabolic stability determinations did not predict in vivo clearance or

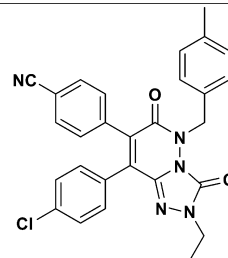
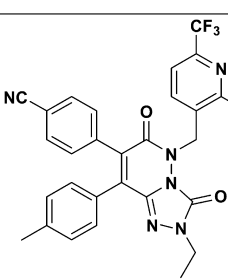
half-life, making it difficult to overcome a major program goal without performing an untenable number of in vivo PK studies.

On the basis of this observation, we analyzed the entire program data set to develop correlations that could be used to predict compounds with shortened in vivo half-life based on in vitro data. There seemed to be little correlation between clearance in vitro and in vivo, as demonstrated in Figure 4A. In vitro and in vivo clearance correlations that factor in free fraction have been reported, and they express in vitro clearance as unbound Cl_{int}.²⁵ These correlations were developed for compounds with log P < 3 and MW < 500,^{26,27} but many of our potent CB1 antagonists are outside of these limits.²⁸ To improve our correlation, we factored in free fraction by using unbound Cl instead of Cl and we filtered the data set to only consider compounds with protein binding ≤95%.²⁹ A trend emerged (Figure 4B) between unbound in vitro metabolism and in vivo clearance in rats. In the process of culling compounds based on free fraction, we plotted *e* log P vs protein binding (Figure 5) and found that compounds in the range of *e* log P 3–4 have a much higher probability of being ≤95% protein bound than compounds with *e* log P > 4.5.

To test the predictive correlation of our model between in vitro clearance and in vivo clearance and half-life, we mined our compound collection to find a derivative in the desired log P range for which we had not yet measured free fraction or clearance. Compound 11 has a measured log P = 3 with 5% free fraction in rat plasma. The unbound in vitro metabolism (0.0063 nmol/min/mg) and in vivo clearance values (iv Cl = 7 mL/min/kg) were in line with predictions and gratifyingly exhibited an anticipated half-life of 3.5 h in rat. To verify the efficacy of the PK/affinity profile of 11 as a CB1 antagonist, compound was administered at 10 mg/kg to rats in an acute feeding model²⁰ wherein reduced feeding was observed at a

Table 4. Methyl Scan of Compound 28 in an Attempt to Introduce a Metabolic Soft-Spot



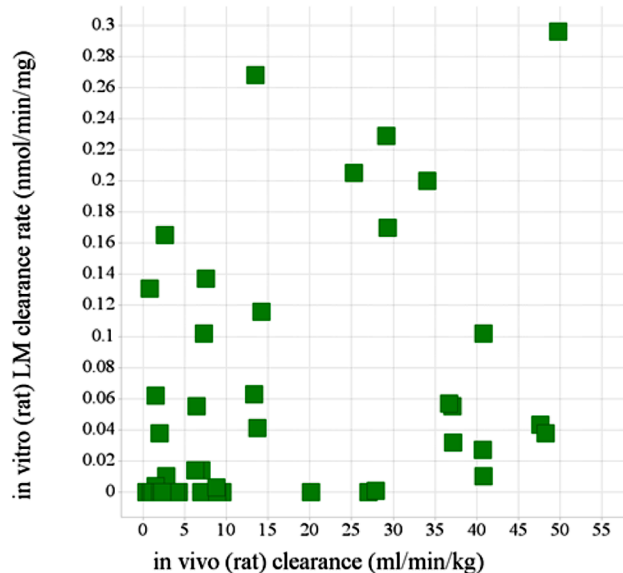
	Cmpd #	<i>h</i> CB1 K _i (nM)	S.D. (nM)	<i>e</i> log P	in vitro Cl (rat) ^a nmol/min/mg	rat T _{1/2} [Cl] mL/min/Kg
R _a =R _b =R _c =R _d =H	28	1.4	0.58	4.6	0.010	7 h [41]
R _a = methyl, others = H	29	3.0	1.3	5.0	0.000	n.d.
R _b = methyl, others = H	30	1.6	0.17	5.0	0.152	n.d.
R _c = methyl, others = H	31	1.9	1.0	5.2	0.014	n.d.
R _d = methyl, others = H	32	1.7	0.77	5.1	0.170	29 h [29]
	33	12	5.8	5.2	n.d.	n.d.
	34	2.9	2.4	4.6	0.052	n.d.

^aIn vitro rat clearance was determined in rat liver microsomes, as described in the Supporting Information. Rat T_{1/2} was not determined for compounds 29–31, 33, and 34.

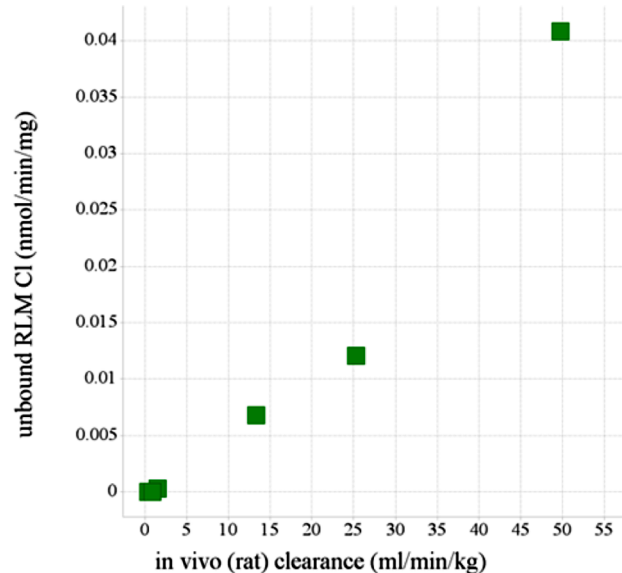
similar level to 10 mg/kg of rimonabant, the positive control in the study.

Using the above criteria, we prospectively considered two compounds with the *e* log P range of 3–4. Compound **35**, with *e* log P = 4.2, had 1% free fraction in rat plasma and demonstrated a shortened half-life (rat, dog, cyno = nd, 45 h, 8 h) relative to benchmark compound **28** (Figure 6). Compound **36**, with *e* log P = 3.6, had 9% free fraction in rat plasma and it also demonstrated a shortened half-life (rat, dog, cyno = 1.1 h,

7 h, 9 h) relative to **28**. Unfortunately, both compounds had liabilities that made them unsuitable for advancement. Compound **35** had poor physicochemical properties, making it difficult to formulate and administer to rats. Compound **36** displayed weak efficacy in the 20 h feeding experiment due to a combination of its short half-life and low plasma and brain exposure over the course of the in vivo experiment. There are many factors beyond clearance that affect in vivo half-life, but these results provided encouragement that compounds with log



4A



4B

Figure 4. (A) In vitro metabolism rate (rat liver microsomes (RLM)) vs rat in vivo Cl (mL/min/kg). (B) Unbound RLM Cl (mL/min/kg) vs rat in vivo Cl (mL/min/kg), filtered to show compounds with $\leq 95\%$ protein binding.

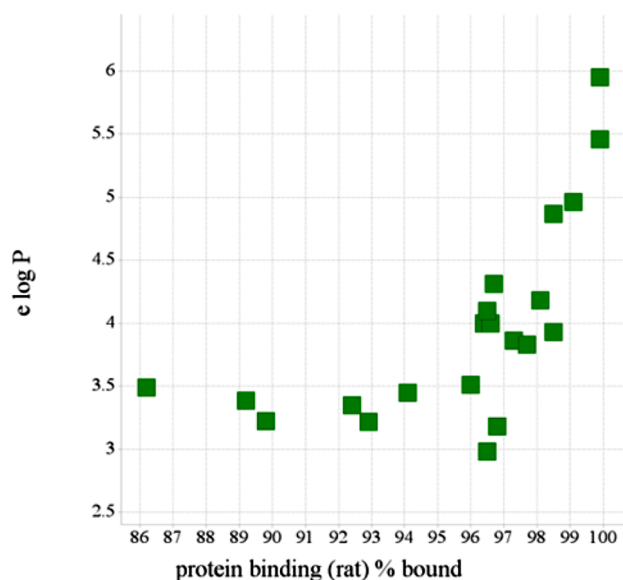


Figure 5. Graph of $e \log P$ vs rat plasma protein binding.

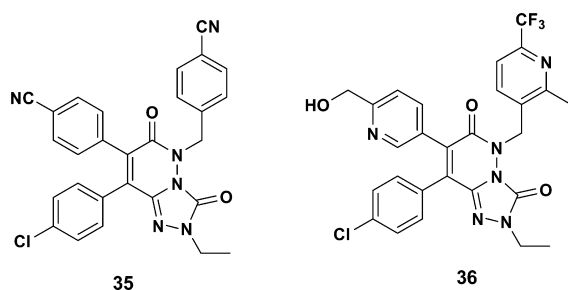


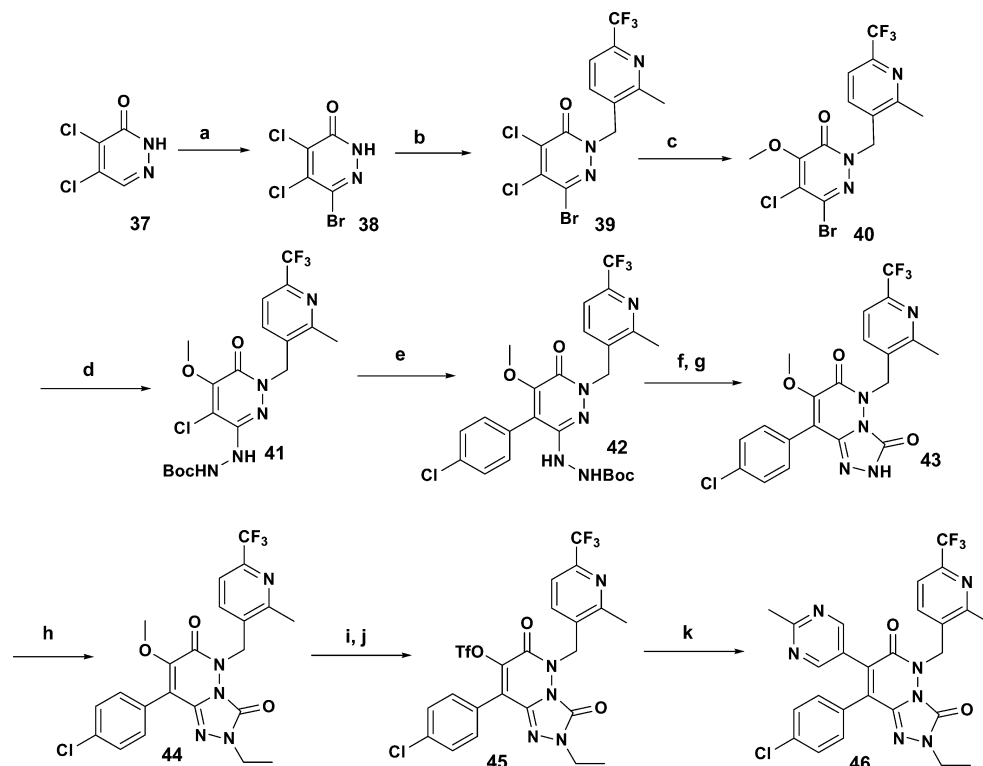
Figure 6. Potent CB1 antagonists ($hCB1 K_i = 5 \text{ nM}$ for both **35** and **36**) with lowered $\log P$ and shortened half-life relative to compound **28**.

P between 3 to 4 could meet the goal of higher free fraction that would bring the possibility of predictable half-life in preclinical species.

With the N2 and N5-substituents of the TZP-dione extensively explored, due in part to their late introduction in the synthesis (steps 5 and 9, Scheme 2), the C7-position remained underexplored despite the experience that polar moieties such as the C7-pyridyl group of compound **15** were tolerated by the CB1 receptor. The synthetic sequence required commitment to the C7 and C8-aryl groups in the first step of the 9-step synthetic sequence (Scheme 2); however, a revised synthesis was developed for late C7 and C8-aryl group introduction, as depicted in Scheme 3, to facilitate the exploration of these substituents.

Dichloropyridazin-one **37** was brominated under basic conditions, followed by selective N-alkylation with **22**, to give pyridazinone **39**. Chlorine displacement with sodium methoxide led to a single regioisomer, **40**. Palladium-catalyzed N-arylation of Boc-hydrazine gave chloride **41** that underwent Suzuki coupling to introduce the C-8 substituent at an intermediate stage in the synthesis. Deprotection of **42** and cyclization with 1,1'-carbonyldiimidazole led to triazolopyridazin-dione **43**. Alkylation of the triazolo-nitrogen with ethyl iodide gave protected triazolopyridazin-dione **44**. Demethylation of the methoxy-group with BBr_3 followed by triflation gave intermediate **45**, enabling introduction of the C7-group in the final step via Suzuki coupling to give **46**.

This revised synthesis enabled a more rapid exploration of the C-7 substituent, targeting compounds with $\log P$ in the range that gave a higher likelihood of having higher free fraction. Compound **47** (Table 5) exhibited significant CYP inhibition, and compounds **48** and **49** exhibited reduced $hCB1$ affinity; however, methylpyrimidine **46** was found to be a potent and selective CB1 antagonist with $e \log P = 3.8$. The compound exhibited reasonable aqueous solubility ($17 \mu\text{g/mL}$) in crystalline form and excellent DMSO/water solubility to enable an accurate in vitro assessment of off-target activities.

Scheme 3. Revised Synthesis of TZP-diones to Enable Late Introduction of C7 and C8-Substituents^a

^a(a) Br₂, LiOH, MeOH; (b) **22**, K₂CO₃, DMF, 80% (2 steps); (c) NaOMe, dioxane, 72%; (d) Pd(dppf)Cl₂, BocNHNH₂, Cs₂CO₃, toluene, 78%; (e) 4-ClPhB(OH)₂, Pd(PPh₃)₄, Na₂CO₃, toluene, 92%; (f) HCl, dioxane; (g) 1,1'-carbonyldiimidazole, THF, 70% (2 steps); (h) EtI, K₂CO₃, DMF, 84%; (i) BBr₃, CH₂Cl₂; (j) Tf₂O, TEA, CH₂Cl₂; (k) Pd(dppf)Cl₂, K₂CO₃, THF, 2-methylpyrimidin-5-boronic acid, 14% (3 steps).

Compound **46** was devoid of CYP inhibition up to 40 μ M, meeting another criterion for advancement. The compound demonstrated high (13% and 7%) free fraction respectively in rat and human plasma, in line with the expectation of significant free fraction. Compound **46** demonstrated low clearance in rat liver microsomes (unbound Cl = 0.0022 nmol/min/mg). However, in vivo clearance was unexpectedly high (43 mL/min/kg), which may have been predicted by its subsequently measured extensive metabolism in rat hepatocytes (5% remaining). Fortunately, this metabolism appeared rat-specific and the compound exhibited the predicted clearance in higher species, leading to a desirable half-life ($T_{1/2}$ = 5, 42, 12 h) and bioavailability (73%, 75%, 51%) in the rat, dog, and cynomolgous monkey, respectively.

Metabolism was the major route of elimination of [¹⁴C]-labeled compound **46** when administered orally at 5 mg/kg to bile duct-cannulated rats. Two major oxidative metabolites containing ¹⁴C-label were observed by LC/MS ([M + 2O – 2H] and [M + O + glucuronide], structures undetermined), and these metabolites accounted for 36% and 26% of the dose, respectively. In comparison, excretion of parent was a minor route of elimination (less than 1% of the dose). Within 48 h post dose, 76% and 7% of the radioactivity was recovered in bile and urine, respectively, with 0.8% of parent radioactivity observed in bile and no parent drug in urine. In rats, therefore, the disposition of compound **46** appears to be primarily mediated by oxidative metabolism, with minimal contribution from direct renal and biliary excretion of the parent compound.

The favorable pharmacokinetic properties of **46**, combined with its potent hCB1 K_i, result in significant reduction in food intake when administered acutely to ad libitum fed rats at 1

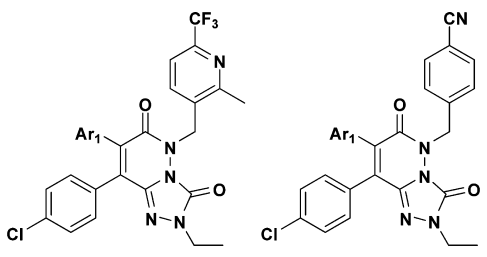
mg/kg. Upon multiple day administration at 3 and 10 mg/kg, **46** caused a statistically significant reduction of body weight over 4 days of 2.8 and 7.2% respectively. Treatment of **46** in a 28-day study in diet-induced obese rats demonstrated body weight reductions of 2.4, 4.1, and 10.2% when administered po at 1, 3, and 10 mg/kg, respectively.²² In this same study, administration of 10 mg/kg of rimonabant produced a 6.2% body weight reduction.

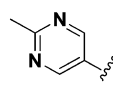
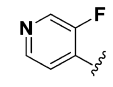
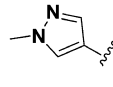
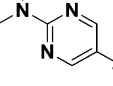
The safety of compound **46** was evaluated both in vitro and in vivo. No off-target liabilities were found despite extensive screening against a panel of GPCRs and ion channels; this may be an added benefit of the reduced log P of the compound.¹⁵ The potential toxicity profile of **46** was evaluated when administered orally to dogs for a 12-day period. The results of the toxicological studies will be described elsewhere; however, the effects observed were consistent with known effects of other CB1 receptor antagonists³⁰ and were not attributed to any off-target liabilities. The findings from the toxicological study, in conjunction with the contemporaneous marketing withdrawal of rimonabant and withdrawals of taranabant and otenabant from clinical development, led to the decision that clinical evaluation of **46** or other centrally acting compounds in this series would not be pursued.

CONCLUSIONS

We report the discovery of a potent, selective CB1 antagonist, compound **46**, which also demonstrates significantly lower log P as compared to other compounds in its class. The lower log P was a critical element in conferring greater free fraction and allowing better predictive in vivo clearance values based on in vitro microsomal metabolism. The introduction of a metabolic

Table 5. CB1 and CYP Isoform SAR of C7-Aryl-triazolopyridazinediones



Ar ₁	Structure	Cmpd #	hCB1 K _i (nM)	S.D. (nM)	<i>e</i> log P	CYP isoform IC ₅₀ (μM)
	A	46	4.7	2.5	3.8	2C19 = >40 2C9 = >40 3A4 = >40
	A	47	3.2	1.7	4.3	2C19 = 5 2C9 = 14 3A4 = 7
	B	48	92	51	3.8	2C19 = >40 2C9 = >40 3A4 = 3.4
	B	49	77	39	4.3	2C19 = >40 2C9 = >40 3A4 = >40

soft spot did not result in compounds with the desired PK profile. A key improvement in the physicochemical properties was achieved when pharmacophoric groups were transposed across an earlier TZP core. A synthetic route was developed that facilitated the introduction of a 2-methyl pyrimidine group that conferred greater polarity to the series while maintaining CB1 antagonist affinity and selectivity. The progression of **46**, and our entire centrally mediated CB1 antagonism program, was halted due to undesired class-related CB1 effects in vivo. We have described herein the methods that accelerated the discovery of potent CB1 antagonists in this series with lower log P and greater free fraction, resulting in more predictable pharmacokinetics and an improved profile against off-target liabilities.

EXPERIMENTAL SECTION

Chemistry. All anhydrous reactions were carried out using oven-dried glassware under an atmosphere of argon or nitrogen. All reagents and solvents were obtained from commercial vendors and used without further purification unless otherwise indicated. NMR spectra (¹H, ¹³C) were recorded on JEOL JNM-ECP500, JEOL GSX400, and Bruker 400 spectrometers. Chemical shifts were given in parts per million (ppm) downfield from internal reference tetramethylsilane standard; coupling constants (*J* values) were given in hertz (Hz).

Elemental analyses were performed by the Bristol-Myers Squibb Discovery Analytical Science Department. Melting points were taken on a Hoover Unimelt melting point apparatus and were uncorrected. LC/MS data were recorded on a Shimadzu LC-10AT equipped with a SIL-10A injector, a SPD-10AV detector normally operating at 220 nm, and interfaced to a Micromass ZMD mass spectrometer. LC/MS or HPLC retention times were reported using a Phenomenex Luna C-18 4.6 mm × 50 mm column eluting with a 4 min gradient of 0–100% solvent B, where solvent A was 10:90:0.1 CH₃OH–H₂O–TFA and solvent B was 90:10:0.1 CH₃OH–H₂O–TFA. Reactions were monitored by TLC using 0.25 mm E. Merck silica gel plates (60 F254) and were visualized using UV light and 5% phosphomolybdic acid in 95% EtOH. All compounds were found to be >95% pure by HPLC analysis unless otherwise noted.

7-(4-Chlorophenyl)-6-methyl-8-(pyridin-4-yl)-2-((6-(trifluoromethyl)pyridin-3-yl)methyl)-[1,2,4]triazolo[4,3-*b*]pyridazin-3(2*H*)-one (4). To a solution of 100 mg (0.2 mmol) of compound **3**¹⁷ in 2 mL of THF at –20 °C was added 0.2 mL of a 3 M solution of methylmagnesium bromide (0.6 mmol). The mixture was stirred for 30 min, and 2 mL of NH₄Cl (satd aq) was added to quench the reaction. The solution was diluted with 40 mL each of EtOAc and satd aq NH₄Cl, and the layers were extracted. The organic layer was dried (Na₂SO₄), filtered, and evaporated to give 100 mg of a yellow oil. The residue was dissolved in 2 mL of CH₂Cl₂, and 47 mg of 2,3-dichloro-5,6-dicyano-*p*-benzoquinone (DDQ, 0.2 mmol) was added. After 15 min at room temperature, the mixture was stored overnight at

–40 °C. The crude reaction mixture was loaded onto silica gel for purification to give 18 mg of a yellow oil that was further purified via preparative RP-HPLC to give 12 mg of compound 4 as a yellow solid (12%). Analytical HPLC (4 min gradient): 2.94 min (97.1% homogeneity index (HI)). HRMS anal. calcd for $C_{24}H_{17}ClF_3N_6O$ [$M + H$]: 497.1104, found 497.1104. 1H NMR (400 MHz, CD_3OD) δ ppm 8.75 (d, $J = 1.8$ Hz, 1H), 8.49 (dd, $J = 1.7, 6.2$ Hz, 2H), 8.04 (dd, $J = 1.8, 8.2$ Hz, 1H), 7.80 (d, $J = 8.2$ Hz, 1H), 7.40–7.23 (m, 6H), 4.85 (s, 2H), 2.29 (s, 3H). ^{13}C NMR (100 MHz, CD_3OD) δ ppm 155.26, 150.84, 150.50, 150.17, 141.34, 139.19, 136.87, 136.50, 136.21, 133.87, 133.12, 132.56, 130.04, 126.26, 121.79, 22.14. ^{19}F NMR (151 MHz, CD_3OD) δ ppm –69.28.

7-(4-Chlorophenyl)-6-methoxy-8-(pyridin-4-yl)-2-((5-(trifluoromethyl)pyridin-2-yl)methyl)-[1,2,4]triazolo[4,3-*b*]pyridazin-3(2H)-one (5). To a solution of compound S6 (71 mg, 0.14 mmol) in methanol (0.3 mL) was added NaOMe (25 wt % in methanol solution) (0.7 mL, 3.2 mmol). The reaction mixture was heated at 50 °C for 20 min, followed by cooling to room temperature and concentration. The residue was diluted with 50 mL each of ethyl acetate and water, and the layers were extracted. The organic layer was separated and dried (Na_2SO_4). The dried organic layer was filtered and concentrated under reduced pressure to give 71 mg (100%) of the title compound as a yellow foam. Analytical HPLC (4 min grad): 3.23 min (99.1% HI). LC-MS anal. calcd for $C_{24}H_{16}ClF_3N_6O_2$: 512.1, found [$M + H$] 512.9. 1H NMR (500 MHz, $CDCl_3$) δ ppm 8.78 (d, $J = 1.6$ Hz, 1H), 8.60–8.56 (m, 2H), 7.95 (dd, $J = 8.0, 1.9$ Hz, 1H), 7.67 (d, $J = 8.2$ Hz, 1H), 7.38–7.27 (m, 2H), 7.17–7.09 (m, 2H), 7.06–6.98 (m, 2H), 5.28 (s, 2H), 4.04 (s, 3H).

7-(4-Chlorophenyl)-8-(pyridin-4-yl)-2-((5-(trifluoromethyl)pyridin-2-yl)methyl)-[1,2,4]triazolo[4,3-*b*]pyridazine-3,6-(2H,5H)-dione (6). To a solution of compound S6 (170 mg, 0.33 mmol) in THF (10 mL) was added potassium trimethylsilanol (169 mg, 1.3 mmol). The reaction mixture was heated to reflux at 85 °C for 1 h. The mixture was cooled to room temperature, and it was concentrated to a thick oil. The residue was diluted with ethyl acetate, and the resulting solution was extracted with water. The organic layer was dried (Na_2SO_4), filtered, and concentrated under reduced pressure. The residue was purified by reverse phase HPLC to give 29 mg (17%) of compound 6 as a yellow solid. Analytical HPLC (4 min gradient) retention time = 3.15 min (97.2% HI). LC-MS anal. calcd for $C_{25}H_{14}ClF_3N_6O_2$: 498.1, found [$M + H$] 499.2. 1H NMR (500 MHz, $DMSO-d_6$) δ ppm 12.93–12.85 (m, 1H), 8.71 (s, 1H), 8.58–8.52 (m, 2H), 7.99–7.88 (m, 2H), 7.40–7.34 (m, 2H), 7.32–7.27 (m, 2H), 7.23–7.17 (m, 2H), 5.31 (s, 2H).

7-(4-Chlorophenyl)-5-methyl-8-(pyridin-4-yl)-2-((5-(trifluoromethyl)pyridin-2-yl)methyl)-[1,2,4]triazolo[4,3-*b*]pyridazine-3,6(2H,5H)-dione (7). To a solution of compound 6 (61 mg, 0.12 mmol) and Li_2CO_3 (28 mg, 0.38 mmol) in DMF (1 mL) was added iodomethane (2.3 mg, 0.16 mmol), and the mixture was stirred at room temperature for 1 h. The resulting mixture was diluted with ethyl acetate, and the resulting solution was washed with water. The organic layer was dried (Na_2SO_4), filtered, and concentrated under reduced pressure. The residue was purified by reverse phase HPLC to give 29 mg (46%) of compound 7 as a light-yellow foam. Analytical HPLC (4 min gradient) retention time = 2.71 min (98.6% HI). LC-MS anal. calcd for $C_{24}H_{16}ClF_3N_6O_2$: 512.1, found [$M + H$] 513.0. 1H NMR (500 MHz, $CDCl_3$) δ ppm 8.74 (s, 1H), 8.68 (br s, 2H), 7.90 (d, $J = 7.7$ Hz, 1H), 7.68 (d, $J = 7.7$ Hz, 1H), 7.39 (br s, 2H), 7.27 (br s, 2H), 7.02 (d, $J = 8.2$ Hz, 2H), 5.14 (s, 2H), 4.12 (s, 3H).

4,4'-(7-(4-Chlorophenyl)-3,6-dioxo-8-(pyridin-4-yl)-[1,2,4]triazolo[4,3-*b*]pyridazine-2,5(3H,6H)-diyl)bis(methylene)dibenzonitrile (8). The title compound (3.6 mg, 22.5% yield) was isolated as a yellow solid as a side-product in the synthesis of compound 10. Analytical HPLC (4 min gradient) retention time = 3.15 min (90.0% HI). LC-MS anal. calcd for $C_{32}H_{20}ClN_7O_2$: 569.1, found [$M + H$] 570.1. 1H NMR (500 MHz, CD_3OD) δ ppm 8.68 (d, $J = 6.6$ Hz, 2H), 7.69 (m, 8H), 7.45 (d, $J = 8.2$ Hz, 2H), 7.35–7.27 (m, 2H), 7.23–7.10 (m, 2H), 5.95 (s, 2H), 5.12 (s, 2H).

3,6-Dichloro-4-(4-chlorophenyl)-5-(pyridin-4-yl)pyridazine (9). Compound 20 (4.9 g crude) was dissolved in 30 mL of $POCl_3$, and the resultant solution was heated to 85 °C for 2 h. The reaction

mixture was cooled to room temperature, and the solution was poured over 600 mL of ice. The slurry was agitated for 30 min, and the pH of the resulting solution was carefully adjusted to pH 5 with cooling as needed. The resulting aqueous slurry was diluted with 400 mL of CH_2Cl_2 , and the layers were extracted. The aqueous layer was re-extracted with 200 mL of CH_2Cl_2 , and the resulting organic layers were combined, washed with brine, dried (Na_2SO_4), filtered, and evaporated to give a black oil. The residue was purified via flash chromatography on silica gel that had been pretreated with 2% TEA/hexanes to give 1.7 g of 9 in 46% yield from 4-pyridylacetic acid. 1H NMR (500 MHz, $CDCl_3$) δ 8.6 (dd, 2H, $J = 1.7, 4.4$ Hz), 7.29 (dt, 2H, $J = 1.7, 8.3$ Hz), 7.02–6.99 (m, 4H).

4-((7-(4-Chlorophenyl)-2-methyl-3,6-dioxo-8-(pyridin-4-yl)-2,3-dihydro-[1,2,4]triazolo[4,3-*b*]pyridazin-5(6H)-yl)methyl)benzonitrile (10). To a solution of compound S4 (8.0 mg, 0.023 mmol) in DMF (0.3 mL) was added K_2CO_3 (5.0 mg, 0.036 mmol), followed by 4-(bromomethyl)benzonitrile (5.0 mg, 0.025 mmol). After 15 min, the reaction mixture was diluted with ethyl acetate, and the resulting solution was washed with water. The organic layer was dried over Na_2SO_4 , filtered, and concentrated under reduced pressure. The crude product was purified by reverse phase HPLC to give 4.2 mg of 4-((7-(4-chlorophenyl)-3,6-dioxo-8-(pyridin-4-yl)-2,3-dihydro-[1,2,4]triazolo[4,3-*b*]pyridazin-5(6H)-yl)methyl)benzonitrile as a yellow foam. Analytical HPLC (4 min gradient) retention time = 2.70 min (96.0% HI). LC-MS anal. calcd for $C_{24}H_{15}ClN_6O_2$: 454.1, found [$M + H$] 455.1. 1H NMR (400 MHz, CD_3OD) δ ppm 8.69 (d, $J = 6.6$ Hz, 2H), 7.84–7.65 (m, 6H), 7.35–7.27 (m, 2H), 7.25–7.07 (m, 2H), 5.95 (s, 2H). A solution of 4-((7-(4-chlorophenyl)-3,6-dioxo-8-(pyridin-4-yl)-2,3-dihydro-[1,2,4]triazolo[4,3-*b*]pyridazin-5(6H)-yl)methyl)benzonitrile (2 mg, 0.004 mmol), methyl iodide (0.001 mL, 1 mg, 0.006 mmol), and K_2CO_3 (2.5 mg, 0.02 mmol) in DMF (0.2 mL) was heated at 80 °C for 2 h. The mixture was cooled to room temperature, and it was filtered and purified by reverse phase HPLC to give 2 mg (90%) of compound 10 as a colorless foam. Analytical HPLC (4 min gradient) retention time = 2.78 min (95.0% HI). LC-MS anal. calcd for $C_{25}H_{17}ClN_6O_2$: 468.1, found [$M + H$] = 469.1. 1H NMR (400 MHz, $CDCl_3$) δ ppm 8.83 (br s, 2H), 7.82–7.64 (m, 4H), 7.61 (d, $J = 4.4$ Hz, 2H), 7.36–7.29 (m, 2H), 7.07 (d, $J = 8.8$ Hz, 2H), 5.98 (s, 2H), 3.58 (s, 3H).

4-((8-(4-Chlorophenyl)-2-methyl-3,6-dioxo-7-(pyridin-4-yl)-2,3-dihydro-[1,2,4]triazolo[4,3-*b*]pyridazin-5(6H)-yl)methyl)benzonitrile (11). To solution of compound S3 (26 mg, 0.064 mmol) in THF (1 mL) was added potassium trimethylsilanol (25 mg, 0.19 mmol), and the mixture was heated to 85 °C for 10 min. The solution was cooled to room temperature, and the pH was adjusted to 7 with 1N HCl. The resulting solution was extracted with ethyl acetate, and the organic layer was extracted with brine. The organic layer was dried ($MgSO_4$), filtered, and concentrated to give 26 mg of a yellow solid that was used as is. A solution of the yellow solid (26 mg, 0.051 mmol), 4-(bromomethyl)benzonitrile (11 mg, 0.056 mmol), and K_2CO_3 (21 mg, 0.15 mmol) in DMF (1 mL) was heated at 80 °C for 10 min, and the mixture was cooled to room temperature. The solution was diluted with ethyl acetate, and the organic layer was extracted with water. The organic layer was dried (Na_2SO_4), filtered, and concentrated under reduced pressure. The crude product was purified by reverse phase HPLC, then treated with 1N HCl to give 15 mg (63%) of compound 11 as yellow solid. Analytical HPLC (4 min gradient) retention time = 2.30 min (98.3% HI). LC-MS anal. calcd for $C_{25}H_{17}ClN_6O_2$: 468.1, found [$M + H$] 469.0. 1H NMR (500 MHz, CD_3OD) δ ppm 8.67 (d, $J = 6.0$ Hz, 2H), 7.81 (d, $J = 6.0$ Hz, 2H), 7.61 (q, $J = 8.2$ Hz, 4H), 7.32–7.05 (m, 4H), 5.84 (s, 2H), 3.44 (s, 3H).

8-(4-Chlorophenyl)-2-methyl-7-(pyridin-4-yl)-5-((6-(trifluoromethyl)pyridin-3-yl)methyl)-[1,2,4]triazolo[4,3-*b*]pyridazine-3,6(2H,5H)-dione (12). Compound 12 was synthesized from compound S5 and 2-trifluoromethyl-5-bromomethylpyridine according to the procedure of compound 10. Analytical HPLC (4 min gradient) retention time = 2.67 min (99.1% HI). HRMS anal. calcd for $C_{24}H_{17}ClF_3N_6O_2$ [$M + H$]: 513.1054, found: 513.1046. 1H NMR (500 MHz, $CDCl_3$) δ ppm 8.96 (d, $J = 1.7$ Hz, 1H), 8.56 (dd, J

= 1.7, 16.1 Hz, 2H), 8.14 (dd, 1.7, 8.3 Hz, 1H), 7.69 (d, J = 8.2 Hz, 1H), 7.31–7.27 (m, 2H), 7.15–7.12 (m, 2H), 7.07–7.05 (m, 2H), 6.03 (s, 2H), 3.59 (s, 3H). ^{13}C NMR (100 MHz, CDCl_3) δ ppm 158.0, 150.9, 149.7, 147.0, 140.4, 138.7, 136.6, 135.9, 134.6, 131.3, 131.2, 129.0, 127.8, 125.2, 120.4, 44.2, 33.7.

8-(4-Chlorophenyl)-2-methyl-5-((2-methyl-6-(trifluoromethyl)pyridin-3-yl)methyl)-7-(pyridin-4-yl)-[1,2,4]-triazolo[4,3-*b*]pyridazine-3,6(2*H*,5*H*)-dione (13). To a solution of compound **S2** (0.17 g, 0.45 mmol) in 0.5 mL of 1,4-dioxane was added a solution of LiOH (38 mg, 0.9 mmol) in 0.5 mL of water. The mixture was stirred, and Bu_4NOH (0.03 mL of 40% solution in water, 0.04 mmol) was added. The resulting mixture was heated in a microwave at 150 °C for 30 min. The mixture was evaporated to dryness and was used as-is in the next step. To a solution of crude 6-chloro-8-(4-chlorophenyl)-2-methyl-7-(pyridin-4-yl)-[1,2,4]triazolo[4,3-*b*]pyridazin-3(2*H*)-one (35 mg, 0.07 mmol) in DMF (0.37 mL) was added compound **22** (15 mg, 0.07 mL) and K_2CO_3 (20 mg, 0.15 mmol). The resulting mixture was heated at 65 °C for 1 h, and then it was cooled to room temperature. The crude reaction mixture was diluted with MeOH, and it was purified via preparative RP-HPLC to give 16 mg of the O-alkylated regioisomer, 8-(4-chlorophenyl)-2-methyl-6-((2-methyl-6-(trifluoromethyl)pyridin-3-yl)methoxy)-7-(pyridin-4-yl)-[1,2,4]triazolo[4,3-*b*]pyridazin-3(2*H*)-one, and 15 mg (38%) of compound **13** as a yellow solid. Analytical HPLC (4 min gradient) retention time = 2.65 min (100% HI). LCMS anal. calcd for $\text{C}_{25}\text{H}_{18}\text{ClF}_3\text{N}_6\text{O}_2$ 526.11, found $[\text{M} + \text{H}]$ 527.2. ^1H NMR (400 MHz, CD_3CN) δ 8.45 (dd, 2H, J = 1.8, 4.4 Hz), 7.79 (d, 1H, J = 7.9 Hz), 7.59 (d, 1H, J = 7.9 Hz), 7.34 (dd, 2H, J = 2.6, 8.4), 7.22 (dd, 2H, J = 2.7, 8.3), 7.11 (dd, 2H, J = 1.8, 4.4 Hz), 5.79 (s, 2H), 3.39 (s, 3H), 2.65 (s, 3H). ^{13}C NMR (100 MHz, CD_3CN) δ 149.6, 136.1, 135.5, 131.9, 128.7, 125.6, 45.1, 33.1, 21.8.

8-(4-Chlorophenyl)-2-ethyl-7-(pyridin-4-yl)-5-((6-(trifluoromethyl)pyridin-3-yl)methyl)-[1,2,4]triazolo[4,3-*b*]pyridazine-3,6(2*H*,5*H*)-dione (14). A solution of 5-(chloromethyl)-2-(trifluoromethyl)pyridine (32 mg, 0.16 mmol) and NaI (27 mg, 0.18 mmol) in DMF (0.5 mL) was stirred at 50 °C for 20 min. The mixture was transferred into a solution of 8-(4-chlorophenyl)-2-ethyl-7-(pyridin-4-yl)-[1,2,4]triazolo[4,3-*b*]pyridazine-3,6(2*H*,5*H*)-dione (70 mg, 0.15 mmol) and LiOH (4 mg, 0.2 mmol) in DMF (0.5 mL). The reaction mixture was heated at 70 °C for 30 min, and then it was cooled to room temperature and diluted with ethyl acetate. The resulting organic layer was extracted with water, and the organic layer was dried (Na_2SO_4), filtered, and concentrated under reduced pressure. The crude product was purified by reverse phase HPLC and silica gel chromatography. The product-containing fractions were evaporated and dissolved in ethyl acetate. The organic layer was extracted with sodium bicarbonate, and then it was dried (Na_2SO_4), filtered, and evaporated to give 6.6 mg (6.6%) of compound **14** as a yellow foam. Analytical HPLC (4 min gradient) retention time = 2.96 min (98.0% HI). LC-MS anal. calcd for $\text{C}_{25}\text{H}_{18}\text{ClF}_3\text{N}_6\text{O}_2$: 526.1, found $[\text{M} + \text{H}]$ 527.2. ^1H NMR (500 MHz, CDCl_3) δ ppm 9.01 (s, 1H), 8.82 (d, J = 4.9 Hz, 2H), 8.21 (d, J = 7.7 Hz, 1H), 7.76 (d, J = 8.2 Hz, 1H), 7.65 (d, J = 4.4 Hz, 2H), 7.38 (d, J = 7.7 Hz, 2H), 7.17 (d, J = 8.2 Hz, 2H), 6.07 (s, 2H), 4.25–3.82 (m, 2H), 1.38 (t, J = 7.4 Hz, 3H).

3-(Chloromethyl)-2-methyl-6-(trifluoromethyl)pyridine (22). A solution of 1 M LAH in THF (40 mL, 40 mmol) was added dropwise to a cooled (0 °C) solution of methyl 2-methyl-6-(trifluoromethyl)nicotinate **25**³¹ (8.8 g, 40 mmol) in 40 mL of dry THF at 0 °C under argon atmosphere. The solution was warmed to room temperature over 1 h. The reaction was slowly quenched with 10% aq Rochelle's salt solution (20 mL) over 10 min, followed by stirring for 1 h. The resulting mixture was diluted with 50 mL of EtOAc and water, and the layers were extracted. The organic phase was dried (Na_2SO_4), filtered, and concentrated to obtain 7.5 g of (2-methyl-6-(trifluoromethyl)pyridin-3-yl)methanol as a colorless oil, which was greater than 98% purity by HPLC/MS. To a solution of (2-methyl-6-(trifluoromethyl)pyridin-3-yl)methanol (14.5 g, 71 mmol) in 100 mL of CH_2Cl_2 at room temperature under argon atmosphere was added SOCl_2 (16.8 g, 142 mmol) and 1.5 mL of DMF. The reaction

solution was stirred for 16 h, followed by evaporation. The residue was dissolved in 200 mL of Et₂O, and the organic layer was extracted with 10% Na_2CO_3 (100 mL), then brine (100 mL). The organic phase was dried (Na_2SO_4), filtered, and concentrated to give 13.7 g (48%) of compound **22** as a tan oil. ^1H NMR (400 MHz, CD_3CN) δ 7.96 (d, 1H, J = 7.7 Hz), 7.64 (d, 1H, J = 7.9 Hz), 4.78 (s, 2H), 2.67 (s, 3H). ^{13}C NMR (100 MHz, CD_3CN) δ 158.4, 146.0 (q, J = 34.0 Hz), 138.3, 134.9, 124.1 (q, CF_3 , J = 275 Hz), 118.2, 42.5, 20.8.

4-(4-Chlorophenyl)-3-(pyridin-4-yl)furan-2(5*H*)-one (18). Potassium *tert*-butoxide (40 mmol; 4.7 g) dissolved in MeOH (20 mL) was added to 4-pyridylacetic acid hydrochloride (20 mmol; 3.5 g) slurried in MeOH (20 mL). After stirring for 15 min, the solvent was removed under reduced pressure and the residue was dissolved in dry DMF (30 mL). To this solution was slowly added 2-bromo-4'-chloroacetophenone (20 mmol; 4.8 g), and the solution turned to a reddish-brown color. After 1 h at room temperature, the reaction mixture was poured into water (200 mL) and this solution was extracted with dichloromethane (2 × 100 mL). The combined organic extracts were dried (MgSO_4), filtered, and concentrated to provide 5.5 g of a dark-green semisolid. The product was slurried in EtOH (~10 mL), and then it was isolated by vacuum filtration and drying under high vacuum to give 3.2 g of **18** (60% yield) as a granular green solid. Analytical HPLC (4 min gradient) retention time = 1.23 min (100.0% HI). LCMS anal. calcd for $\text{C}_{15}\text{H}_{10}\text{ClNO}_2$ 271.04, found $[\text{M} + \text{H}]$ 272. ^1H NMR (400 MHz, CDCl_3) δ 8.6 (dd, 1.6, 4.6 Hz, 2H), 7.38–7.23 (m, 6H), 5.18 (s, 2H). ^{13}C NMR (100 MHz, CDCl_3) δ 171.9, 157.7, 150.4, 137.9, 137.6, 129.7, 128.8, 128.4, 124.3, 123.6, 114.6, 70.6.

4-(4-Chlorophenyl)-5-(pyridin-4-yl)pyridazine-3,6-diol (20). Compound **18** (3 g, 11 mmol) was dissolved in 550 mL of THF, and potassium *tert*-butoxide (2.5 g, 28 mmol, 2 equiv) was added. Air was bubbled through the solution with vigorous stirring, and the reaction mixture turned from red to dark-green within a few minutes. When starting material had disappeared, as monitored by HPLC, the reaction was quenched via addition of excess (>3 equiv) 1N HCl. The mixture was stirred for 1 h and evaporated to give **19** as a dark-green oil. The residue was dissolved in 50 mL of ethanol, and 0.35 mL of hydrazine (11 mmol, 1 equiv) was added, followed by 3 mL of conc HCl. The reaction mixture was heated to 72 °C for 18 h and, after cooling, the mixture was evaporated to give 4.9 g of **20** as a red foam that was used as-is in the next step.

6-Chloro-5-(4-chlorophenyl)-4-(pyridin-4-yl)pyridazin-3(2*H*)-one (21, As a Mixture of Isomers). To a solution of compound **9** (11 g, 32.7 mmol) in 100 mL of acetonitrile was added 100 mL of 1N NaOH (aq). The mixture was heated at 65 °C for 2 h, and the reaction was quenched via addition of 1N HCl to pH 6. A precipitate formed that was collected and suction dried to give 7.8 g (75%) of a beige solid as a 8:1 mixture of regioisomers. Analytical HPLC (4 min gradient) retention time = 2.07 min (88.3% HI). ^1H NMR (400 MHz, CD_3CN) δ major isomer: 8.60 (d, J = 6.8 Hz, 2H), 7.78 (d, J = 6.8 Hz, 2H), 7.58–7.36 (m, 2H), 7.22–7.17 (m, 2H), 2.05 (br s, 1H); minor isomer: 8.70 (d, J = 6.8 Hz, 2H), 7.87 (d, J = 6.8 Hz, 2H), 7.36–7.26 (m, 2H), 7.14–7.12 (m, 2H), 2.05 (br s, 1H).

6-Chloro-5-(4-chlorophenyl)-2-((2-methyl-6-(trifluoromethyl)pyridin-3-yl)methyl)-4-(pyridin-4-yl)-pyridazin-3(2*H*)-one (23). To a solution of compound **21** (7.6 g, 24 mmol) in 100 mL of DMF was added K_2CO_3 , and the mixture was heated to 65 °C. To the heated mixture was added a solution of compound **22** (6.0 g, 29 mmol) in DMF (10 mL) in three portions over 2 h. After 45 min, the mixture was poured into 800 mL of water and 500 mL of EtOAc was added. The layers were extracted, and the organic layer was successively washed with 500 mL each of water and brine. The organic layer was dried (Na_2SO_4), filtered, and evaporated to give a red oil. The residue was purified via silica gel chromatography to give 7.8 g (66%) of **23** as beige crystals (the minor regioisomer is removed during silica purification). Analytical HPLC (4 min gradient) retention time = 3.37 min (100.0% HI). ^1H NMR (400 MHz, CDCl_3) δ 8.57–8.43 (m, 2H), 7.96 (d, J = 7.9 Hz, 1H), 7.54 (d, J = 7.9 Hz, 1H), 7.35–7.19 (m, 2H), 7.07–6.91 (m, 4H), 5.45 (s, 2H), 2.83 (s, 3H).

8-(4-Chlorophenyl)-5-((2-methyl-6-(trifluoromethyl)pyridin-3-yl)methyl)-7-(pyridin-4-yl)-[1,2,4]triazolo[4,3-*b*]pyridazine-3,6(2*H*,5*H*)-dione (24). To a solution of compound 23 (6.6 g, 13 mmol) in pyridine (25 mL) was added 6 mL of hydrazine (130 mmol), and the mixture was heated in a microwave at 200 °C for 30 min. The reaction mixture was evaporated to give a light-yellow foam that was dissolved in THF (140 mL). To this solution was added 1,1'-carbonyldiimidazole (2.2 g, 13 mmol), and the solution was heated to 65 °C for 1 h. The crude reaction mixture was purified over silica gel to give 5.0 g of compound 24 as an orange foam (73% from 23). Analytical HPLC (4 min gradient) retention time = 2.37 min (100.0% HI). ¹H NMR (400 MHz, CD₃CN) δ 8.56–8.40 (m, 2H), 7.85 (d, *J* = 7.8 Hz, 1H), 7.69–7.49 (m, 1H), 7.43–7.32 (m, 2H), 7.32–7.21 (m, 2H), 7.20–7.09 (m, 2H), 7.04 (s, 1H), 5.83 (s, 2H), 2.69 (s, 3H).

8-(4-Chlorophenyl)-2-ethyl-5-((2-methyl-6-(trifluoromethyl)pyridin-3-yl)methyl)-7-(pyridin-4-yl)-[1,2,4]triazolo[4,3-*b*]pyridazine-3,6(2*H*,5*H*)-dione (15). To a mixture of compound 24 (5.0 g, 9.8 mmol) and K₂CO₃ (1.6 g, 12 mmol) in DMF (50 mL) was added a solution of ethyl iodide (0.8 mL) in DMF (3 mL), and the mixture was stirred at room temperature for 3 h. The reaction mixture was diluted with 1 L of water, and the resulting milky solution was extracted with 2 × 500 mL of EtOAc. The combined organic layers were washed successively with water, 10% Na₂S₂O₃, and brine. The organic layer was dried (Na₂SO₄), filtered, and evaporated to give 4.0 g of a brown foam. The material was purified via silica gel chromatography to give 3.6 g of compound 15 as a yellow foam (67%). Recrystallization of 1.4 g of this material provided 1.2 g (90% recovery) of off-white crystals. Analytical HPLC (4 min gradient) retention time = 2.89 min (100.0% HI). HRMS anal. calcd for C₂₆H₂₁N₆O₂ClF₃ [M + H]: 541.1370, found: 541.1361. ¹H NMR (600 MHz, DMSO-*d*₆) δ ppm 8.49 (d, 2H, *J* = 4.9 Hz), 7.95 (d, 1H, *J* = 8.1 Hz), 7.73 (d, 1H, *J* = 8.1 Hz), 7.44 (d, 2H, *J* = 8.5 Hz), 7.30 (d, 2H, *J* = 8.5 Hz), 7.16 (d, 2H, *J* = 4.9 Hz), 5.72 (s, 2H), 3.80 (q, 2H, *J* = 7.2 Hz), 2.64 (s, 3H), 1.18 (t, 3H, *J* = 7.2 Hz). ¹³C NMR (150 MHz, DMSO-*d*₆) δ ppm 158.5, 156.6, 149.6, 146.5, 144.5 (q, *J* = 33.9 Hz), 141.5, 141.6, 136.2, 135.8, 135.6, 135.5, 134.7, 132.2, 131.9, 129.7, 128.9, 125.8, 122.2 (q, *J* = 274 Hz), 118.7 (q, *J* = 2 Hz), 45.7, 41.3, 22.3, 14.1. ¹⁹F NMR (376.46 MHz, DMSO-*d*₆) δ ppm –66.68. Elemental Anal. Calcd for C₂₆H₂₀N₆O₂Cl F₃: C 57.71, H 3.76, N 15.48, Cl 6.53, F 10.50. Found: C 57.73, H 3.69, N 15.53, Cl 6.60, F 11.12.

8-(4-Chlorophenyl)-2-ethyl-5-((2-methyl-6-(trifluoromethyl)pyridin-3-yl)methyl)-7-(2-methylpyridin-4-yl)-[1,2,4]triazolo[4,3-*b*]pyridazine-3,6(2*H*,5*H*)-dione (27). Compound 27 was synthesized according to the method of compound 15. Analytical HPLC (4 min gradient) retention time = 2.462 min (98% HI), LC-MS anal. calcd for C₂₇H₂₂ClF₃N₆O₂: 554.1, found [M + H] = 555.2. ¹H NMR (500 MHz, CDCl₃) δ 8.34 (d, *J* = 5.5 Hz, 1H), 7.64–7.42 (m, 2H), 7.24 (d, *J* = 8.2 Hz, 2H), 7.13 (d, *J* = 8.8 Hz, 2H), 6.91 (s, 1H), 6.74 (d, *J* = 4.9 Hz, 1H), 5.86 (s, 2H), 3.85 (q, *J* = 7.1 Hz, 2H), 2.67 (s, 3H), 2.44 (s, 3H), 1.26 (t, *J* = 7.1 Hz, 3H). ¹³C NMR (126 MHz, CDCl₃) δ 158.5, 158.1, 157.0, 148.9, 146.5, 146.3, 136.5, 136.1, 135.2, 135.0, 133.0, 131.3, 128.9, 128.0, 124.8, 122.3, 118.0, 45.0, 41.8, 24.4, 22.4, 13.8.

4-(8-(4-Chlorophenyl)-2-ethyl-5-((2-methyl-6-(trifluoromethyl)pyridin-3-yl)methyl)-3,6-dioxo-2,3,5,6-tetrahydro-[1,2,4]triazolo[4,3-*b*]pyridazin-7-yl)benzonitrile (28).³² Compound 28 (35 mg, 80% yield) was isolated as a light-yellow solid. Analytical HPLC (4 min gradient) retention time = 3.67 min (98.7% HI). LCMS anal. calcd C₂₈H₂₀ClF₃N₆O₂: 564.13, found [M + H] = 565. ¹H NMR (400 MHz, CDCl₃) δ 7.65 (d, *J* = 7.91 Hz, 1H), 7.57 (d, *J* = 8.35 Hz, 2H), 7.51 (d, *J* = 7.91 Hz, 1H), 7.31 (d, *J* = 8.35 Hz, 2H), 7.22–7.28 (m, 2H), 7.18 (d, *J* = 8.79 Hz, 2H), 5.93 (s, 2H), 3.92 (q, *J* = 7.18 Hz, 2H), 2.74 (s, 3H), 1.34 (t, *J* = 7.25 Hz, 3H).

4-(8-(4-Chlorophenyl)-2-ethyl-5-((2-methyl-6-(trifluoromethyl)pyridin-3-yl)methyl)-3,6-dioxo-2,3,5,6-tetrahydro-[1,2,4]triazolo[4,3-*b*]pyridazin-7-yl)-2-methylbenzonitrile (29).³² Analytical HPLC (4 min gradient) retention time = 3.79 min (98.7% HI). LCMS anal. calcd C₂₉H₂₂ClF₃N₆O₂: 578.14, found [M + H] = 579. ¹H NMR (400 MHz, CDCl₃) δ ppm 7.63 (d, *J* = 8.1 Hz, 1H), 7.58–7.42 (m, 2H), 7.38–7.28 (m, 2H), 7.22–7.11 (m, 3H),

6.99 (d, *J* = 7.1 Hz, 1H), 5.93 (s, 2H), 3.92 (q, *J* = 7.3 Hz, 2H), 2.74 (s, 3H), 2.47 (s, 3H), 1.33 (t, *J* = 7.2 Hz, 3H).

4-(8-(4-Chlorophenyl)-2-ethyl-5-((2-ethyl-6-(trifluoromethyl)pyridin-3-yl)methyl)-3,6-dioxo-2,3,5,6-tetrahydro-[1,2,4]triazolo[4,3-*b*]pyridazin-7-yl)benzonitrile (30).³² Compound 30 was isolated in 47% yield as a light-yellow solid. Analytical HPLC (4 min gradient) retention time = 3.82 min (98.6% HI). LCMS anal. calcd C₂₉H₂₂ClF₃N₆O₂: 578.14, found [M + H] = 579. ¹H NMR (400 MHz, CDCl₃) δ 7.61 (d, *J* = 7.91 Hz, 1H), 7.57 (d, *J* = 8.79 Hz, 2H), 7.49 (d, *J* = 7.91 Hz, 1H), 7.31 (d, *J* = 8.79 Hz, 2H), 7.23–7.28 (m, 2H), 7.18 (d, *J* = 8.79 Hz, 2H), 5.98 (s, 2H), 3.93 (q, *J* = 7.18 Hz, 2H), 3.03 (q, *J* = 7.47 Hz, 2H), 1.35 (td, *J* = 7.31, 12.63 Hz, 6H).

4-(8-(4-Chlorophenyl)-2-isopropyl-5-((2-methyl-6-(trifluoromethyl)pyridin-3-yl)methyl)-3,6-dioxo-2,3,5,6-tetrahydro-[1,2,4]triazolo[4,3-*b*]pyridazin-7-yl)benzonitrile (31).³² Compound 31 was isolated in 66% yield as a light-yellow solid. Analytical HPLC (4 min gradient) retention time = 3.81 min (95.6% HI). LCMS anal. calcd C₂₉H₂₂ClF₃N₆O₂: 578.14, found [M + H] = 579. ¹H NMR (400 MHz, CDCl₃) δ 7.66 (d, *J* = 8.35 Hz, 1H), 7.57 (d, *J* = 8.35 Hz, 2H), 7.51 (d, *J* = 8.35 Hz, 1H), 7.30 (d, *J* = 8.79 Hz, 2H), 7.23–7.27 (m, 2H), 7.13–7.21 (m, 2H), 5.93 (s, 2H), 4.53 (quin, *J* = 6.70 Hz, 1H), 2.74 (s, 3H), 1.35 (d, *J* = 7.03 Hz, 6H).

4-(8-(4-Chlorophenyl)-5-((2-methyl-6-(trifluoromethyl)pyridin-3-yl)methyl)-3,6-dioxo-2-propyl-2,3,5,6-tetrahydro-[1,2,4]triazolo[4,3-*b*]pyridazin-7-yl)benzonitrile (32).³² Compound 32 was isolated in 45% yield as a light-yellow solid. Analytical HPLC (4 min gradient) retention time = 3.82 min (100% HI). LCMS anal. calcd C₂₉H₂₂ClF₃N₆O₂: 578.14, found [M + H] = 579. ¹H NMR (400 MHz, CDCl₃) δ 7.64 (d, *J* = 7.91 Hz, 1H), 7.57 (d, *J* = 8.35 Hz, 2H), 7.50 (d, *J* = 7.91 Hz, 1H), 7.31 (d, *J* = 8.79 Hz, 2H), 7.24–7.28 (m, 2H), 7.17 (d, *J* = 8.35 Hz, 2H), 5.94 (s, 2H), 3.78–3.87 (m, 2H), 2.74 (s, 3H), 1.76 (sxt, *J* = 7.38 Hz, 2H), 0.91 (t, *J* = 7.47 Hz, 3H).

4-(8-(4-Chlorophenyl)-2-ethyl-5-(4-methylbenzyl)-3,6-dioxo-2,3,5,6-tetrahydro-[1,2,4]triazolo[4,3-*b*]pyridazin-7-yl)benzonitrile (33).³² Compound 33 (40 mg, 100%) was isolated as a yellow solid. Analytical HPLC (4 min gradient) retention time = 3.90 min (97.5% HI). LCMS anal. calcd for C₂₈H₂₂ClN₅O₂: 495.1, found [M + H] 496.4. ¹H NMR (400 MHz, CD₃CN) δ ppm 7.64–7.57 (m, 2H), 7.34 (d, *J* = 7.9 Hz, 2H), 7.32–7.26 (m, 4H), 7.21–7.13 (m, 4H), 5.80 (s, 2H), 3.84 (q, *J* = 7.2 Hz, 2H), 2.30 (s, 3H), 1.29–1.19 (m, 3H).

4-(2-Ethyl-5-((2-methyl-6-(trifluoromethyl)pyridin-3-yl)methyl)-3,6-dioxo-8-(*p*-tolyl)-2,3,5,6-tetrahydro-[1,2,4]triazolo[4,3-*b*]pyridazin-7-yl)benzonitrile (34).³² Compound 34 was isolated in 50% yield as a light-yellow solid. Analytical HPLC (4 min gradient) retention time = 3.64 min (96.7% HI). LCMS anal. calcd for C₂₉H₂₃F₃N₆O₂: 544.18, found [M + H] 545. ¹H NMR (400 MHz, CDCl₃) δ 7.65 (d, *J* = 7.91 Hz, 1H), 7.54 (d, *J* = 8.35 Hz, 2H), 7.51 (d, *J* = 7.91 Hz, 1H), 7.20–7.31 (m, 2H), 7.12 (s, 4H), 5.93 (s, 2H), 3.92 (q, *J* = 7.03 Hz, 2H), 2.74 (s, 3H), 2.35 (s, 3H), 1.33 (t, *J* = 7.03 Hz, 3H).

4-(8-(4-Chlorophenyl)-5-(4-cyanobenzyl)-2-ethyl-3,6-dioxo-2,3,5,6-tetrahydro-[1,2,4]triazolo[4,3-*b*]pyridazin-7-yl)benzonitrile (35).³² Compound 35 (70 mg, 52%) was isolated as a yellow solid. Analytical HPLC (4 min gradient) retention time = 3.55 min (98.3% HI). LC-MS anal. calcd for C₂₈H₁₉ClN₆O₂: 506.1, found [M + H] 507.2. ¹H NMR (400 MHz, CD₃CN) δ ppm 7.79–7.69 (m, 2H), 7.65–7.56 (m, 4H), 7.36–7.26 (m, 4H), 7.24–7.15 (m, 2H), 5.85 (s, 2H), 3.84 (q, *J* = 7.3 Hz, 2H), 1.31–1.19 (m, 3H).

8-(4-Chlorophenyl)-2-ethyl-7-(6-(hydroxymethyl)pyridin-3-yl)-5-((2-methyl-6-(trifluoromethyl)pyridin-3-yl)methyl)-[1,2,4]triazolo[4,3-*b*]pyridazine-3,6(2*H*,5*H*)-dione (36). To a stirred solution of 8-(4-chlorophenyl)-2-ethyl-5-((2-methyl-6-(trifluoromethyl)pyridin-3-yl)methyl)-7-(6-methylpyridin-3-yl)-[1,2,4]triazolo[4,3-*b*]pyridazine-3,6(2*H*,5*H*)-dione³² (140 mg, 0.24 mmol) in CH₂Cl₂ (2 mL) was added mCPBA (65 mg of 77% mCPBA, 0.29 mmol) at room temperature. After stirring for 1 h, the solution was diluted with ethyl acetate and the organic layer was extracted with satd aq NaHCO₃. The organic layer was separated and dried (MgSO₄). The dried organic layer was filtered and concentrated

to give a colorless foam that was dissolved in CH_2Cl_2 (2 mL), and trifluoroacetic anhydride (2 mL) was added. The vessel was sealed and heated to 50 °C for 2 h. The reaction mixture was cooled to room temperature and was evaporated to an oil. The residue was purified via preparative RP-HPLC; product-containing fractions were evaporated and redissolved in CH_2Cl_2 and water that was adjusted to pH 8 with solid NaHCO_3 . The layers were extracted and the organic layer was dried (MgSO_4), filtered, and evaporated to give 56 mg (36%) of compound **36** as a yellow solid. Analytical HPLC (8 min gradient) retention time = 4.0 min (100% HI). anal. calcd for $\text{C}_{27}\text{H}_{22}\text{ClF}_3\text{N}_6\text{O}_3$ 570.14, found $[\text{M} + \text{H}]$ 571.5. ^1H NMR (400 MHz, CDCl_3) δ 8.26 (d, 1H, $J = 2.2$ Hz), 7.64 (d, 1H, $J = 7.7$), 7.55 (dd, 1H, $J = 2.2, 8.2$), 7.50 (d, 1H, $J = 7.7$), 7.33–7.20 (m, 6H), 5.94 (s, 2H), 4.73 (s, 2H), 3.93 (q, 2H, $J = 7.1$), 2.74 (s, 3H), 1.33 (t, 3H, $J = 7.1$ Hz). ^{13}C NMR (100 MHz, CDCl_3) δ 159.4, 158.6, 156.9, 149.9, 146.4, 139.1, 136.4, 135.9, 135.3, 135.0, 133.0, 131.5, 130.2, 129.0, 128.2, 127.1, 119.6, 118.0, 64.0, 53.4, 45.0, 41.8, 22.3, 13.7.

6-Bromo-4,5-dichloropyridazin-3(2H)-one (38).³³ To a solution of 20 g of 4,5-dichloropyridazin-3(2H)-one (121 mmol) in methanol at 70 °C was added 5 g of LiOH (121 mmol), followed by slow portionwise addition of bromine (14 mL, 270 mmol). To the heated solution was added 3 g of LiOH until the solution became light-red/orange. The volatile components were removed in vacuo, and the resulting slurry was suspended in 150 mL of water. The solids were collected via filtration, and the filter cake was washed with water and suction dried to give 30 g of a beige solid that was used without further purification.

6-Bromo-4,5-dichloro-2-((2-methyl-6-(trifluoromethyl)pyridin-3-yl)methyl)pyridazin-3(2H)-one (39). To a heated (70 °C) solution of compound **38** (17 g, 69 mmol) in 100 mL of DMF containing 19 g of K_2CO_3 (140 mmol) was added a solution of compound **22** (14 g, 69 mmol) in DMF (100 mL). The solution was heated for 2 h, and the mixture was cooled to room temperature. The resulting solution was diluted into 1.5 L of water. The mixture was extracted with 2×600 mL of ethyl acetate. The combined organic layers were washed with brine, and then it was dried (MgSO_4), filtered, and evaporated to give 25 g of a red solid that was used without further purification.

6-Bromo-5-chloro-4-methoxy-2-((2-methyl-6-(trifluoromethyl)pyridin-3-yl)methyl)pyridazin-3(2H)-one (40). The residue (25 g of crude compound **39**) was dissolved in NaOMe/MeOH (6.5 g of a 25% w/w solution, 30 mmol) at room temperature. After 15 min, the mixture was diluted into 500 mL of $\text{EtOAc}/\text{water}$. The layers were extracted, and the organic layer was washed with brine. The organic layer was separated and dried (MgSO_4), filtered, and evaporated to give a red oil that was purified via silica gel chromatography to give 4.0 g (35%) compound **40** as a white solid. Analytical HPLC (4 min gradient) retention time = 3.66 min (97.6% HI). LCMS anal. calcd for $\text{C}_{13}\text{H}_{10}\text{BrClF}_3\text{N}_3\text{O}_2$: 411, 413, 415, found $[\text{M} + \text{H}] = 412, 414, 416$. ^1H NMR (400 MHz, CDCl_3) δ 7.7 (d, 8.0 Hz, 1H), 7.5 (d, 8.0 Hz, 1H), 5.3 (s, 2H), 4.31 (s, 3H), 2.75 (s, 3H). ^{13}C NMR (100 MHz, CDCl_3) δ 158.2, 155.8, 152.1, 147.3, 138.0, 132.0, 129.8, 125.7, 123.0 (app q, CF_3), 118.1 (d, 2.8 Hz), 61.1, 52.1, 22.5.

tert-Butyl 2-(4-Chloro-5-methoxy-1-((2-methyl-6-(trifluoromethyl)pyridin-3-yl)methyl)-6-oxo-1,6-dihydropyridazin-3-yl)hydrazinecarboxylate (41). To an argon flushed vessel containing 3.7 g of compound **40** (9 mmol), boc-hydrazine (4.7 g, 36 mmol), and cesium carbonate (3.5 g, 11 mmol) in toluene (45 mL) was added $\text{Pd}(\text{dppf})\text{Cl}_2$ -methylene chloride complex (0.37 g, 0.45 mmol), and the mixture was heated at reflux for 4 h. The cooled mixture was diluted with 200 mL each of ethyl acetate and water. The layers were extracted, and the organic layer was washed successively with 1N HCl and brine. The organic layer was dried (MgSO_4), and the mixture was filtered and evaporated to give a red oil that was purified via silica gel chromatography to give 3.2 g (77%) of compound **41** as an orange foam. Analytical HPLC (4 min gradient) retention time = 3.21 min (91.3% HI). ^1H NMR (500 MHz, CDCl_3) δ 7.6 (d, 7.7 Hz, 1H), 7.44 (d, 8.0 Hz, 1H), 6.47 (br s, 1H), 5.24 (s, 2H), 4.29 (s, 3H), 2.74 (s, 3H), 1.48 (m, 9H). ^{13}C NMR (125 MHz, CDCl_3) δ 157.8,

155.6, 155.4, 151.8, 146.7, 144.5, 137.4, 133.1, 118.0, 81.8, 60.7, 51.1, 28.2, 28.0, 22.4.

tert-Butyl 2-(4-(4-Chlorophenyl)-5-methoxy-1-((2-methyl-6-(trifluoromethyl)pyridin-3-yl)methyl)-6-oxo-1,6-dihydropyridazin-3-yl)hydrazinecarboxylate (42). To a solution of compound **41** (1.5 g, 3.23 mmol) in 16 mL of toluene was added 0.76 g of 4-chlorophenyl boronic acid (4.9 mmol) and 1.9 mL of 2 M Na_2CO_3 (3.9 mmol). The mixture was degassed via vacuum/Ar purge sequence three times, and $\text{Pd}(\text{PPh}_3)_4$ (0.19 g, 0.16 mmol) was added. The resulting mixture was heated at 110 °C for 85 min. After cooling to room temperature, the mixture was diluted with 300 mL each of ethyl acetate/water, and the layers were extracted. The organic layer was washed with brine, then it was dried (MgSO_4), filtered, and evaporated. The residue was purified via silica gel chromatography to give 1.8 g of compound **42** as a beige solid. Analytical HPLC (4 min gradient) retention time = 1.90 min (94.1% HI). LCMS anal. calcd for $\text{C}_{24}\text{H}_{25}\text{ClF}_3\text{N}_5\text{O}_4$ 539, found $[\text{M} + \text{H}]$ 540. ^1H NMR (400 MHz, CDCl_3) δ 7.73 (d, 8 Hz, 1H), 7.49–7.46 (m, 4H), 7.33 (d, 7.4 Hz, 1H), 6.1 (br s, 1H), 5.5 (d, 4.1 Hz, 1H), 5.3 (s, 2H), 4.0 (s, 3H), 2.8 (s, 3H), 1.48–1.39 (m, 9H).

8-(4-Chlorophenyl)-7-methoxy-5-((2-methyl-6-(trifluoromethyl)pyridin-3-yl)methyl)-[1,2,4]triazolo[4,3-b]pyridazine-3,6(2H,5H)-dione (43). Compound **42** (1.8 g, 3.3 mmol) was dissolved in 16 mL of CH_2Cl_2 , and 2 mL of TFA was added. After stirring at room temperature for 4.5 h, the mixture was evaporated to dryness to give an orange oil. The residue was dissolved in 100 mL of CH_2Cl_2 , and the mixture was extracted successively with 1N aq NaOH and brine. The organic layer was dried (MgSO_4), filtered, and evaporated to a yellow foam. The solids were dissolved in 16 mL of CH_2Cl_2 , and triphosgene (3 g, 10 mmol) was added. The slurry was further diluted with 1 mL of CH_2Cl_2 to re-establish stirring, and 0.3 g of triphosgene was added. After 2 h, the mixture was diluted with CH_2Cl_2 and water, and the layers were extracted. The organic layer was washed with brine, and then it was dried (MgSO_4), filtered, and evaporated to give 1.2 g of compound **43** as a white solid. ^1H NMR (400 MHz, CD_3CN) δ 10.2 (s, 1H), 7.75 (d, 8.0 Hz, 1H), 7.65–7.54 (m, 5H), 5.78 (s, 2H), 3.89 (s, 3H), 2.69 (s, 3H). ^{13}C NMR (125 MHz, CD_3CN) δ 162.1, 161.9, 153.4, 140.3, 136.9, 133.7, 132.6, 128.5, 66.1, 50.2, 26.8.

8-(4-Chlorophenyl)-2-ethyl-5-((2-methyl-6-(trifluoromethyl)pyridin-3-yl)methyl)-7-(2-methylpyrimidin-5-yl)-[1,2,4]triazolo[4,3-b]pyridazine-3,6(2H,5H)-dione (46). To a solution of compound **43** (1.0 g 2 mmol) in 2 mL of CH_2Cl_2 at –40 °C was added 2 mL of 1N BBr_3 in CH_2Cl_2 (2 mmol). After 15 min, the mixture was diluted with 100 mL of CH_2Cl_2 and the mixture was extracted with an aq soln of Rochelle's salt. The layers were extracted, and the organic layer was washed with brine. The organic layer was dried (MgSO_4), and then it was filtered and evaporated to give 0.62 g of a brown oil. The residue was dissolved in 6.5 mL of CH_2Cl_2 at 0 °C, and to this solution was added triethylamine (0.36 mL, 2.6 mmol) and triflic anhydride (0.33 mL, 1.9 mmol). After 15 min, the mixture was diluted into 50 mL of CH_2Cl_2 and 50 mL of 0.1 N aq HCl. The layers were extracted, and the organic layer was washed with brine. The organic layer was dried (MgSO_4), and it was filtered and evaporated to give 0.7 g of compound **45** as a red oil that was used as-is in the next step. Compound **45** (0.15 g, 0.24 mmol), 2-methylpyrimidine-5-boronic acid (0.05 g, 0.36 mmol), $\text{Pd}(\text{dppf})\text{Cl}_2\text{-CH}_2\text{Cl}_2$ complex (0.04 g, 0.05 mmol), and K_3PO_4 (0.16 g, 0.73 mmol) were placed in a flask that was then evacuated and purged with argon three times. To the vessel was added 1.2 mL of THF, and the mixture was heated at 80 °C for 3 h. The mixture was allowed to stand at room temperature overnight, followed by dilution with 50 mL each of ethyl acetate and water. The layers were extracted, and the organic layer was washed with brine. The organic layer was dried (MgSO_4), and then it was filtered and evaporated to give a red oil. The residue was purified via silica gel chromatography (using silica that had been pretreated with 2% triethylamine/hexanes) to give 0.03 g of the title compound as a light-yellow solid. Analytical HPLC (4 min gradient) retention time = 3.42 min (100% HI). LCMS Anal. calcd for $\text{C}_{26}\text{H}_{21}\text{N}_7\text{O}_2\text{F}_3\text{Cl}$ 555.14, found 556.2 $[\text{M} + \text{H}]$. ^1H NMR (400 MHz, $\text{DMSO}-d_6$) δ ppm 8.45 (s,

2H), 7.94 (d, 1H, $J = 8.0$ Hz), 7.72 (d, 1H, $J = 8.0$ Hz), 7.50 (d, 2H, $J = 8.8$ Hz), 7.37 (d, 2H, $J = 8.6$ Hz), 5.75 (s, 2H), 3.81 (q, 2H, $J = 7.3$ Hz), 2.65 (s, 3H), 2.57 (s, 3H), 1.18 (t, 3H, $J = 7.2$ Hz). ^{13}C NMR (100 MHz, CDCl_3) δ ppm 166.4, 158.3, 157.9, 156.1, 145.9, 144.0 (q, $J = 33.6$ Hz), 135.6, 135.4, 135.1, 134.8, 134.3, 131.9, 129.1, 128.5, 127.9, 124.3, 121.6 (q, $J = 273.6$), 118.2 (d, $J = 3.1$ Hz), 45.2, 40.8, 25.3, 21.7, 13.5. ^{19}F NMR (471 MHz, $\text{DMSO}-d_6$) δ ppm -66.10 (br s, 3 F). Elemental analysis: Anal. calcd for $\text{C}_{26}\text{H}_{21}\text{N}_7\text{O}_2\text{F}_3\text{Cl}$ C 56.17, H 3.81, N 17.64, Cl 6.38, F 10.25. Found: C 56.01, H 4.01, N 17.24, Cl 6.16, F 10.25.

In Vitro CB1 Binding Assay. The source of CB1 receptor was a membrane preparation from Chinese hamster ovary (CHO) cells overexpressing recombinant human CB1. This CHO–CB1 cell line was in-licensed from Euroscreen (cell line EC-110-C) and expresses a high level of CB1 receptor. Compound **46** and other test compounds were serially diluted in DMSO and added 1:100 to 96 well microtiter plates containing 3 μg of CHO–CB1 membrane protein and 2–5 nM of the cannabinoid small molecule agonist, $[\text{^3H}]$ -CP-55940, or the CB1 selective small molecule antagonist, $[\text{^3H}]$ -rimonabant, in a binding buffer (25 mM HEPES (pH 7.4), 150 mM NaCl, 1 mM EDTA, 2 mM MgCl_2 , 0.25% BSA, 1 mM leupeptin). Incubations were carried out to steady state for 3 h at room temperature for $[\text{^3H}]$ -CP-55940 or 1.5 h for $[\text{^3H}]$ -rimonabant. Binding reactions were terminated by rapid vacuum filtration through GF/B filter plates which were washed with 1.6 mL of 1.8 mM Na_2HPO_4 , 0.9 mM NaH_2PO_4 (pH 7.4), 32.5 mM NaCl, with 0.025% Tween 20, dried, and 0.05 mL of Microscint 20 was added to each well and radioactivity quantified on a Packard TopCount scintillation counter. Nonspecific binding was determined by the addition of 1–10 μM of unlabeled CP-55940 or rimonabant. Specific binding CPM were calculated by subtracting nonspecific binding from total binding. Specific CPM were converted into % inhibition values, and IC_{50} values were determined by nonlinear regression curve fitting carried out in Excel Fit. IC_{50} values were converted into K_i values employing the Cheng–Prusoff correction using the parameters of radioligand concentration and the K_d values determined for each radioligand. K_i values are reported as the average of at least three determinations with calculated standard deviations. Rimonabant was included in all radioligand binding experiments as an internal reference. Saturation (Scatchard) analyses were carried out to determine the dissociation constant, K_d of the radioligands.

The K_d and B_{max} values determined for the two radioligands in membranes from a CHO–huCB1 cell line from Euroscreen are as follows: $[\text{^3H}]$ -CP-55940, $K_d = 6.8$ nM, $B_{\text{max}} = 18$ pmol/mg protein; $[\text{^3H}]$ -rimonabant, $K_d = 2.2$ nM, $B_{\text{max}} = 5.2$ pmol/mg protein. The K_d values obtained with both radioligands are similar to those reported in the literature.³⁴

■ ASSOCIATED CONTENT

● Supporting Information

Experimental procedures for the synthesis of compounds **47**–**49** and **S1**–**S6**, methods for in vitro and in vivo biological studies, and data used to generate graphs in Figures 4A,B and Figure 5 may be found in the Supporting Information section. This material is available free of charge via the Internet at <http://pubs.acs.org>.

■ AUTHOR INFORMATION

Corresponding Author

*Phone: +1-609-818-4965. Fax: +1-609-818-3550. E-mail: Bruce.Ellsworth@BMS.com.

Notes

The authors declare no competing financial interest.

■ ACKNOWLEDGMENTS

We thank Jeffrey Robl, Ph.D., for helpful suggestions in the preparation of this manuscript.

■ ABBREVIATIONS USED

CB1, cannabinoid receptor 1; hCB1, human CB1 receptor; GPCR, G-protein coupled receptor; 2-AG, 2-arachidonoylglycerol; PK, pharmacokinetic; HTS, high-throughput screening; TZP, triazolopyridazine; TZP-dione, triazolopyridazin-dione; MED, minimally efficacious dose; Cl, clearance; CYP, cytochrome P450

■ REFERENCES

- (1) Piomelli, D.; Giuffrida, A.; Calignano, A.; Rodriguez de Fonseca, F. The Endocannabinoid System as a Target for Therapeutic Drugs. *Trends Pharmacol. Sci.* **2000**, *21*, 218–224.
- (2) (a) Rinaldi-Carmona, M.; Barth, F.; Heaulme, M.; Shire, D.; Calandra, B.; Congy, C.; Martinez, S.; Maruani, J.; Neliat, G.; Caput, D.; Ferrara, P.; Soubrie, P.; Breliere, J. C.; Le Fur, G. SR141716A, a Potent and Selective Antagonist of the Brain Cannabinoid Receptor. *FEBS Lett.* **1994**, *350*, 240–244. (b) Mukhopadhyay, S.; Howlett, A. C. Chemically Distinct Ligands Promote Differential CB₁ Cannabinoid Receptor-Gi Protein Interactions. *Mol. Pharmacol.* **2005**, *67*, 2016–2024.
- (3) (a) Pi-Sunyer, F. X.; Aronne, L. J.; Heshmati, H. M.; Devin, J.; Rosenstock, J. Effect of Rimonabant, a Cannabinoid-1 Receptor Blocker, on Weight and Cardiometabolic Risk Factors in Overweight or Obese Patients. *JAMA, J. Am. Med. Assoc.* **2006**, *295*, 761–775. (b) Van Gaal, L. F.; Rissanen, A. M.; Scheen, A. J.; Ziegler, O.; Rössner, S. Effects of the Cannabinoid-1 Receptor Blocker Rimonabant on Weight Reduction and Cardiovascular Risk Factors in Overweight Patients: 1-Year Experience from the RIO-Europe Study. *Lancet* **2005**, *365*, 1389–1397. (c) Bellocchio, L.; Mancini, G.; Vicennati, V.; Pasquali, R.; Pagotto, U. Cannabinoid Receptors as Therapeutic Targets for Obesity and Metabolic Diseases. *Curr. Opin. Pharmacol.* **2006**, *6*, 586–591.
- (4) Walthion, N. European Medicines Agency Press Release EMEA/39457/2009, January 30, 2009; and, European Medicines Agency Press Release EMEA/537153/2008, October 23, 2008.
- (5) Seltzman, H. H. Recent CB1 Cannabinoid Receptor Antagonists and Inverse Agonists. *Drug Dev. Res.* **2009**, *70* (8), 601–615.
- (6) Letourneau, J. J.; Joki, P.; Olson, J.; Riviello, C. M.; Ho, K.-K.; McAleer, L.; Yang, J.; Swanson, R. N.; Baker, J.; Cowley, P.; Edwards, D.; Ward, N.; Ohlmeyer, M. H. J.; Webb, M. L. Identification and Hit-to-lead Optimization of a Novel Class of CB1 Antagonists. *Bioorg. Med. Chem. Lett.* **2010**, *20*, 5449–5453.
- (7) Griffith, D. A.; Hadcock, J. R.; Black, S. C.; Iredale, P. A.; Carpino, P. A.; DaSilva-Jardine, P.; Day, R.; DiBrino, J.; Dow, R. L.; Landis, M. S.; O'Connor, R. E.; Scott, D. O. Discovery of 1-[9-(4-Chlorophenyl)-8-(2-chlorophenyl)-9H-purin-6-yl]-4-ethylaminopiperidine-4-carboxylic Acid Amide Hydrochloride (CP-945,598), a Novel, Potent, and Selective Cannabinoid Type 1 Receptor Antagonist. *J. Med. Chem.* **2009**, *52*, 234–237.
- (8) Rimonabant: Acomplia EPAR Product Information; European Agency for The Evaluation of Medicinal Products: London, 2009; http://www.ema.europa.eu/ema/index.jsp?url=pages/medicines/human/medicines/000666/human_med_000623.jsp&mid=WC0b01ac058001d124.
- (9) Addy, C.; Rothenberg, P.; Li, S.; Majumdar, A.; Agrawal, N.; Li, H.; Zhong, L.; Yuan, J.; Maes, A.; Dunbar, S.; Cote, J.; Rosko, K.; Van Dyck, K.; De Lepeleire, I.; de Hoon, J.; Van Hecken, A.; Depre, M.; Knops, A.; Gottesdiener, K.; Stoch, A.; Wagner, J. Multiple-Dose Pharmacokinetics, Pharmacodynamics, and Safety of Taranabant, a Novel Selective Cannabinoid-1 Receptor Inverse Agonist, in Healthy Male Volunteers. *J. Clin. Pharmacol.* **2008**, *48*, 734–744.
- (10) Miao, Z.; Sun, H.; Liras, J.; Prakash, C. Excretion, Metabolism, and Pharmacokinetics of 1-(8-(2-Chlorophenyl)-9-(4-chlorophenyl)-9H-purin-6-yl)-4-(ethylamino)piperidine-4-carboxamide, a Selective Cannabinoid Receptor Antagonist, in Healthy Male Volunteers. *Drug Metab. Dispos.* **2012**, *40* (3), 568–578.
- (11) Greenblatt, D. J. Elimination Half-life of Drugs: Value and Limitations. *Annu. Rev. Med.* **1985**, *36*, 421–427.

- (12) Welling, P. G. *Pharmacokinetics*; ACS Monograph 185; American Chemical Society: Washington, DC, 1986; pp 187–200.
- (13) Salzman, C.; Shader, R. I.; Greenblatt, D. J.; Harmatz, J. S. Long v Short Half-life Benzodiazepines in the Elderly. *Arch. Gen. Psychiatry* **1983**, *40*, 293–297.
- (14) Ellsworth, B. A.; Wang, Y.; Zhu, Y.; Pendri, A.; Gerritz, S. W.; Sun, C.; Carlson, K. E.; Kang, L.; Baska, R. A.; Yang, Y.; Huang, Q.; Burford, N. T.; Cullen, M. J.; Johnghar, S.; Behnia, K.; Pelleymounter, M. A.; Washburn, W. N.; Ewing, W. R. Discovery of Pyrazine Carboxamide CB1 Antagonists: The Introduction of a Hydroxyl Group Improves the Pharmaceutical Properties and In Vivo Efficacy of the Series. *Bioorg. Med. Chem. Lett.* **2007**, *17*, 3978–3982.
- (15) Meanwell, N. A. Improving Drug Candidates by Design: A Focus on Physicochemical Properties As a Means of Improving Compound Disposition and Safety. *Chem. Res. Toxicol.* **2011**, *24* (9), 1420–1456.
- (16) Yu, G.; Ellsworth, B. A.; Mikkilineni, A.; Wu, X.; Wang, Y.; Sitkoff, D.; Gu, Z.; Murugesan, N.; Swartz, S.; Carlson, K. E.; Kang, L.; Yang, Y.; Lee, N.; Baska, R. A.; Huang, Q.; Cullen, M. J.; Zuvich, E.; Thomas, M.; Rohrbach, K.; Devenny, J.; Godonis, H.; Harvey, S.; Johnghar, S.; Behnia, K.; Pelleymounter, M. A.; Ewing, W. R. Discovery of Di-Aryl Triazolopyridazine Cannabinoid Receptor (CB1) Antagonists. Fall 2008 ACS National Meeting, Philadelphia, PA, August 17–21, 2008, MEDI 010, .
- (17) Yang, Y.; Miller, K. J.; Zhu, Y.; Hong, Y.; Tian, Y.; Murugesan, N.; Gu, Z.; O'Tanyi, E.; Keim, W. J.; Rohrbach, K. W.; Johnghar, S.; Behnia, K.; Pelleymounter, M. A.; Carlson, K. E.; Ewing, W. R. Characterization of a novel and selective CB1 antagonist as a radioligand for receptor occupancy studies. *Bioorg. Med. Chem. Lett.* **2011**, *21* (22), 6856–6860.
- (18) The regiochemistry of Grignard addition that we report herein appears to be previously unreported; however, Grignard reagents are found to add to pyridazin-3(2H)-ones as reported in: Verhelst, T.; Verbeeck, S.; Ryabtsova, O.; Depraetere, S.; Maes, B. U. W. Synthesis of Functionalized Pyridazin-3(2H)-ones via Nucleophilic Substitution of Hydrogen (SnH). *Org. Lett.* **2011**, *13*, 272–275.
- (19) Experimental log P “e log P” was determined by the HPLC method, as described in: Valko, K.; Bevan, C.; Reynolds, D. Chromatographic Hydrophobicity Index by Fast-Gradient RP-HPLC: A High-Throughput Alternative to log P/log D. *Anal. Chem.* **1997**, *69*, 2022–2029.
- (20) Rohrbach, K. W.; Han, S.; Gan, J.; O'Tanyi, E. J.; Zhang, H.; Chi, C. L.; Taub, R.; Largent, B. L.; Cheng, D. Disconnection Between the Early Onset Anorectic Effects by C75 and Hypothalamic Fatty Acid Synthase Inhibition in Rodents. *Eur. J. Pharmacol.* **2005**, *511*, 31 Where indicated, % reduction in food intake is recorded at a shorter timepoint..
- (21) For experimental details, see: Sitkoff, D. F.; Lee, N.; Ellsworth, B. A.; Huang, Q.; Kang, L.; Baska, R.; Huang, Y.; Sun, C.; Pendri, A.; Malley, M. F.; Scaringe, R. P.; Gougoutas, J. Z.; Reggio, P. H.; Ewing, W. R.; Pelleymounter, M. A.; Carlson, K. E. Cannabinoid CB₁ Receptor Ligand Binding and Function Examined Through Mutagenesis Studies of F200 and S383. *Eur. J. Pharmacol.* **2011**, *651* (1–3), 9–17.
- (22) Methods and results described in: Azzara, A.; Behnia, K.; Cullen, M. J.; Devenny, J.; Ellsworth, B.; Ewing, W.; Glick, S.; Godonis, H.; Harvey, S.; Keim, W.; Murugesan, N.; Rohrbach, K.; Thomas, M.; Pelleymounter, M. A. The Novel Cannabinoid-1 Receptor Antagonists BMS-812204 and BMS-811064 Reduce Food Intake and Body Weight in Preclinical Models of Obesity. Obesity Society 27th Annual Scientific Meeting, Washington, DC, October 24–28, 2009, Poster 750-P.
- (23) Bioavailability was determined from a comparison of exposures from iv vs oral administration of compound; clearance was determined from the terminal time points of the plasma profile upon iv administration. %F in rat, dog, and cynomologous monkey: 50, 40, and 15%, respectively. Clearance in rat, dog, and cynomologous monkey: 10, 12, 31 mL/min/kg. Intravenous elimination half-life in rat, dog, and cynomologous monkey: 5, 38, and 6 h, respectively.
- (24) Compound **28** displays 3 µg/mL aqueous solubility from an amorphous form and immeasurable solubility from a crystalline form.
- (25) Riley, R. J.; McGinnity, D. F.; Austin, R. P. A Unified Model for Predicting Human Hepatic, Metabolic Clearance from in Vitro Intrinsic Clearance Data in Hepatocytes and Microsomes. *Drug Metab. Dispos.* **2005**, *33*, 1304–1311.
- (26) Parrott, N.; Paquereau, N.; Coassolo, P.; Lave, T. An Evaluation of the Utility of Physiologically Based Models of Pharmacokinetics in Early Drug Discovery. *J. Pharm. Sci.* **2005**, *94*, 2327–2343.
- (27) Tamaki, S.; Komura, H.; Kogayu, M.; Yamada, S. Comparative Assessment of Empirical and Physiological Approaches on Predicting Human Clearances. *J. Pharm. Sci.* **2011**, *100*, 1147–1155.
- (28) The physicochemical characteristics of ligands for lipophilic GPCRs have been reviewed in Vieth, M.; Sutherland, J. J. Dependence of Molecular Properties on Proteomic Family for Marketed Oral Drugs. *J. Med. Chem.* **2006**, *49*, 3451.
- (29) Masimirembwa, C. M.; Bredberg, U.; Andersson, T. B. Metabolic Stability for Drug Discovery and Development. *Clin. Pharmacokinet.* **2003**, *42* (6), 515–528.
- (30) Davis-Bruno, K. Non-clinical Overview: CNS Toxicity with Rimonabant; U.S. Food and Drug Administration Center for Drug Evaluation and Research: Silver Spring, MD, June 13, 2007; www.fda.gov/ohrms/dockets/ac/07/slides/2007-4306s1-09-FDA-Bruno.ppt.
- (31) Okada, E.; Kinomura, T.; Higashiyama, Y.; Takeuchi, H.; Hojo, M. A Simple and Convenient Synthetic Method for Alpha-Trifluoromethylpyridines. *Heterocycles* **1997**, *46*, 129–132.
- (32) Synthesized according to the method described in: Wu, G.; Sher, P.; Ellsworth, B. A.; Wu, X.; Ewing, W. R. Manuscript in preparation.
- (33) Kazimierczuk, Z.; Kaminshi, J.; Flavio, M. Studies on Improved Synthesis of 2'-Deoxyribonucleosides of Pyridazine Derivatives. *Collect. Czech. Chem. Commun.* **2006**, *71* (6), 889–898.
- (34) Howlett, A. C.; Barth, F.; Bonner, T. I.; Cabral, G.; Casellas, P.; Devane, W. A.; Felder, C. C.; Herkenham, M.; Mackie, K.; Martin, B. R.; Mechoulam, R.; Pertwee, R. G. International Union of Pharmacology. XXVII. Classification of Cannabinoid Receptors. *Pharmacol. Rev.* **2002**, *54*, 161–202.